# GEOLOGIC FRAMEWORK DERIVED FROM HIGH-RESOLUTION SEISMIC REFLECTION, SIDE-SCAN SONAR, AND VIBRACORE DATA OFFSHORE OREGON INLET TO DUCK, DARE COUNTY, NORTH CAROLINA


Stephen K. Boss

*Department of Geosciences*

*113 Ozark Hall*

*University of Arkansas*

*Fayetteville, AR  72701*

and

Charles W. Hoffman

*Coastal Plain Office*

*North Carolina Geological Survey*

*1620 Mail Service Center*

*Raleigh, NC  27699-1620, NC*



Prepared for

U. S. Minerals Management Service

International Activities and Marine Minerals Division (INTERMAR)

Under Cooperative Agreement 14-12-0001-30348

Draft Submitted: February 2001

Final Report:  June 2001

## EXECUTIVE SUMMARY

Digital seismic profile data collected offshore of the northern Outer Banks, North Carolina were processed and interpreted to delineate principal reflecting horizons and develop a three-dimensional seismic stratigraphic framework for the insular continental shelf between Oregon Inlet and Duck, North Carolina. Developments in Geographic Information System technology over the past few years made it possible to derive gridded data from a network of intersecting, two-dimensional seismic profiles to provide three-dimensional images of reflecting horizons and seismic stratigraphic units (Boss and Hoffman, 2000). This methodology provides high-quality digital 3-D images of selected horizons of the offshore stratigraphy to be displayed on desktop computers or plotted on large format maps.

Data were analyzed from twenty-three single-channel, high-resolution seismic reflection profiles arranged in an orthogonal grid with profiles spaced at two nautical mile intervals over an area of 338 square nautical miles (1,138 $km^2$). Eight profiles were oriented parallel with the existing shoreline between Oregon Inlet and Duck, North Carolina and thirteen profiles were oriented perpendicular to shore. Two additional profiles were run diagonally across the grid.

Interpretation of these data indicated five principal reflecting horizons were present within the upper 60 m of the shelf stratigraphic succession. The uppermost seismic stratigraphic unit (unit $S_1$) represented sedimentary deposits resulting from extensive fluvial incision of the continental shelf during an episode (or episodes) of lowered sea-level. Fluvial processes during development of unit $S_1$ were responsible for extensive erosion, reworking, and re-deposition of sediment throughout most of the northern half of the study area. Three-dimensional mapping of unit $S_1$ and its basal reflector (designated $R_1$) clearly demonstrates the origin of this deposit by fluvial systems traversing eastward across the continental shelf.

The remaining four stratigraphic units (designated $S_2$ – $S_5$) display generally tabular depositional geometry, low total relief, and thicken toward the east-southeast as their basal reflectors dip gently at gradients between 0.75 m/nautical mile ($0.02^{\circ}$) and 1.0 m/nautical mile ($0.03^{\circ}$). Several stratigraphic units ($S_2$ and $S_3$) were truncated and removed by fluvial erosion/deposition throughout much of the northern half of the study area during development of unit $S_1$. Remnants of $S_2$ and $S_3$ were found in interfluvial divides, however. The depositional environment of these units was not determined, but several cores penetrated unit $S_2$ and indicated a sand-prone depositional setting. Deeper stratigraphic units were not sampled by vibracores, so no direct information regarding their composition was available.

Five seafloor types were defined by the acoustic character of the seafloor observed on analog side-scan sonar records: 1) a weak acoustic return producing a generally uniform, featureless sonar record; 2) a moderate to strong acoustic return produced by seafloor sediments with stronger acoustic backscatter characteristics; 3) seafloor with mixed weak and strong acoustic backscatter producing a “patchwork” pattern; 4) seafloor with overall weak acoustic backscatter but with small areas of stronger backscatter producing a characteristic “speckled” appearance on sonar records; 5) potential “hard-bottom” or “live-bottom” identified by the presence of small scarps evident on the side-scan sonar records.

Textural analyses of fifty-six vibracores acquired within the study area revealed that sediments are composed of two dominant lithofacies, designated Type I and Type II. Type I lithofacies were sand-prone, and were subdivided into four sub-facies based on specific textural characteristics. Type II lithofacies were mud-prone, and were subdivided into two sub-facies based on specific textural characteristics. Significantly, sand-prone cores were all located on bathymetric highs believed to have developed as shoals during the Holocene. Mud-prone lithofacies were all developed within the boundaries of the paleofluvial system, indicating that these sediments formed primarily as back-filling estuarine deposits during transgression.

Knowledge of the subsurface stratigraphic architecture in three dimensions enhances the scientific understanding of the development of continental shelf depositional successions, especially offshore North Carolina where such data are relatively sparse. In addition, archiving of these data in a GIS makes them compatible with other data from the continental shelf and enhances the ability of scientists, resource managers, and decision-makers to analyze relationships among different data sets.

This study refined an earlier assessment of sand resources in the Outer Continental Shelf (OCS) area off Dare County. Four potential borrow sites are identified with a total estimated volume of 306 million cubic yards. More detailed study will be needed to more precisely delineate higher and lesser grade material and sand that is more or less suitable for nourishment application within these more general areas. These and mining limitations, such as water depth or environmental restrictions, may reduce the ultimate sand resource volume. Nevertheless, there is a significant quantity of sand in the OCS off Dare County, North Carolina.

## INTRODUCTION

The U. S. Minerals Management Service (MMS) has the responsibility for administering the Department of the Interior's role in activities associated with mineral resource development on the Nation's Outer Continental Shelf (OCS). The OCS is a zone that generally extends from 3- miles seaward of the coastal state boundaries out to 200 miles. The MMS negotiates with a State or local government for a noncompetitive lease for OCS sand and gravel for shore protection, beach or wetland restoration, or use in other construction projects funded or authorized by the Federal government.

The Federal OCS is expected to be a long-term source of sand for coastal erosion management because of the general diminishing supply of onshore and nearshore sand, the renourishment cycles for beaches or coastal areas requiring quantities of sand not currently available from State sources, and the need for large quantities of sand for immediate/emergency repair of beach and coastal damage from severe coastal storms. All beach nourishment/storm protection projects sponsored in whole or in part by the Federal Government require a 50-year supply of sand to complete the full cycle of each project. There appears to be a plentiful supply of clean, high-quality sand within Federal waters off the U.S. coastal states; the depth limits of dredging technologies are evolving such that it becomes more economically feasible to use these deposits every year.

The Outer Banks is experiencing very high rates of erosion which is affecting one of the State's premiere tourist attractions. The State has an established policy of beach nourishment as the preferred option for beach stabilization. Sand management is an important environmental and economic issue in North Carolina. The 93 miles of shoreline from Cape Hatteras to the Virginia line average 4.7 feet of erosion per year. Annual rates for selected segments of developed beachfront property exceed 10 feet per year. The MMS has been closely working with the State of North Carolina to locate suitable sources of sand and environmental studies are underway to ensure that development of these resources is done in an environmentally sound manner.

During the summer of 1994, the United States Minerals Management Service (MMS) authorized the North Carolina Geological Survey (NCGS) to acquire marine geophysical data (single-channel, high-resolution seismic reflection and side-scan sonar profiles) in waters under federal jurisdiction offshore Oregon Inlet northward to Duck (Fig. 1). The surveyed area extended from nearshore, approximately 1 nautical mile seaward of the beach (approximately 1.85 km) at Oregon Inlet northward approximately 26 nautical miles (48.1 km) to Duck, NC and seaward for fifteen nautical miles (27.8 km; Fig. 1). Survey data were collected on an orthogonal survey grid. Eight tracklines were oriented parallel to shore and spaced seaward from shore at 2-nautical mile (3.7 km) intervals between Oregon Inlet and Duck. Thirteen tracklines were oriented perpendicular to shore at two nautical mile spacing between Oregon Inlet and Duck and extended seaward to the limit of the survey area. Two additional tracklines were surveyed diagonally northeast to southwest across the primary grid to provide additional tie points. This resulted in a total of twenty-three geophysical tracklines constituting approximately 346 nautical miles (640 km) in an area of 338 square nautical miles (1,338 $km^2$).

In addition to geophysical data, the NCGS obtained fifty-six vibracores within the study area during the summer of 1996. The maximum length of individual vibracores was six meters (limited by the length of core barrel that could be fitted to the vibracoring rig) and a total of approximately 300 m of core was obtained. These cores were transported to the core repository of the Coastal Plain Office of NCGS where they were cut, split, sampled, described, photographed, and archived.

The purpose of this report is to describe the geological framework of the study area derived from interpretation of both seismic reflection and side-scan sonar data integrated with sediment textural data derived from analyses of vibracores. In particular, interpretation of seismic reflection profiles were used to construct a three-dimensional perspective of the geologic framework of this portion of the continental shelf by delineating the primary seismic reflecting horizons and mapping those horizons within a Geographic Information System (GIS). Display of these data using three-dimensional visualization software provides insight into the geologic history and process stratigraphy of the insular continental shelf related to Quaternary sea-level fluctuations and the response of sedimentary systems to changing base level.

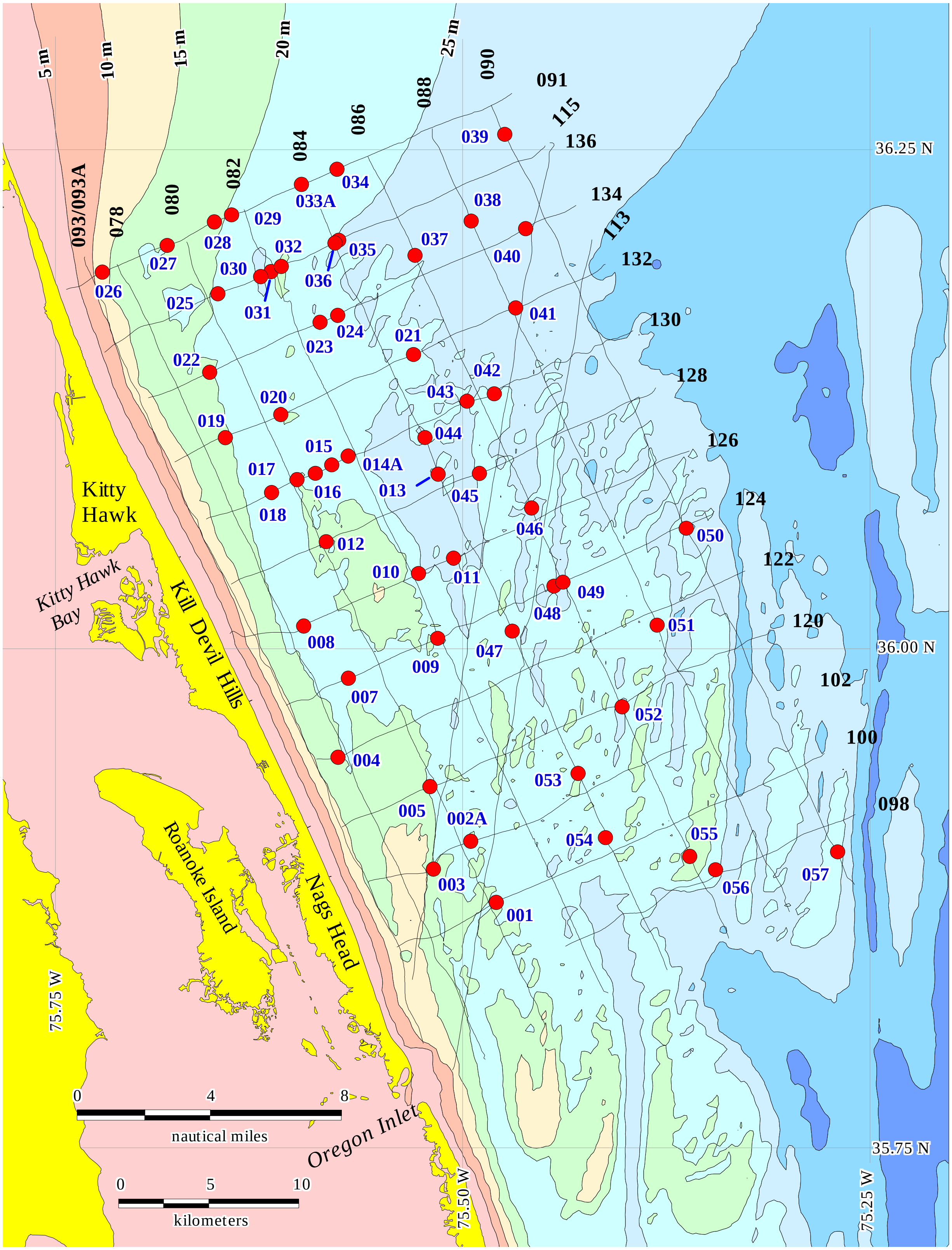


Figure 1. Location map showing the project study area offshore of Dare County, North Carolina and the distribution of seismic and side scan sonar ship track lines (black lines) and vibracore locations (red filled circles). Contour interval is 5 meters.

## Previous Work

Previous work relevant to the study area was mostly conducted by Stanley R. Riggs (East Carolina University), his collaborators, and students during the last three decades (Riggs, 1996; Riggs et al., 1995; Riggs et al., 1992; Schlee et al., 1988; Riggs and Belknap, 1988; Eames, 1983; Bellis et al., 1975; Riggs and O'Connor, 1974; O'Connor et al., 1973). A number of studies concentrated on the Quaternary evolution of depositional environments within the Albemarle estuarine system west of the modern barrier island complex (Bellis et al., 1975; Eames, 1983; O'Connor et al. 1973; Riggs, 1996; Riggs et al., 1992; Riggs and O'Conner, 1974; York et al. 1989). Several other studies focused on identification and mapping of stratigraphic units and seafloor characteristics on the insular continental shelf immediately offshore of the modern barrier island complex (Boss and Hoffman, 2000; Boss and Hoffman, 1999a-d; Boss et al., 1999; Hoffman, 1998; Snyder, 1993) of the North Carolina Outer Banks.

From the earliest works onward, it was recognized that stratigraphic relationships within this portion of the North Carolina coastal plain/continental shelf were spatially complex owing to the very low gradient, low relief geomorphology (Riggs and O'Connor, 1974; Schlee et al, 1988; Riggs and Belknap, 1988; Riggs et al. 1992) and the Quaternary history of large amplitude sea-level oscillations (Fairbanks, 1989). In particular, sea-level oscillations during the Quaternary resulted in multiple regressions and transgressions of the distal coastal plain and continental shelf of North Carolina. During each regressive interval, fluvial systems reestablished, and incised into coastal plain and continental shelf sediments, and eroded sediments resulting from previous depositional episodes (Fig. 2).

During subsequent transgression, fluvial valleys were inundated by rising sea-level and the locus of fluvial sedimentation stepped landward many tens of kilometers, creating estuarine systems dominated by deposition of organic-rich mud and coastal barrier island and shallow marine shelf environments dominated by fine to medium sand reworked from fluvial deposits (Riggs et al., 1992; Riggs, 1996; Riggs and Belknap, 1988). The result of numerous sea- level

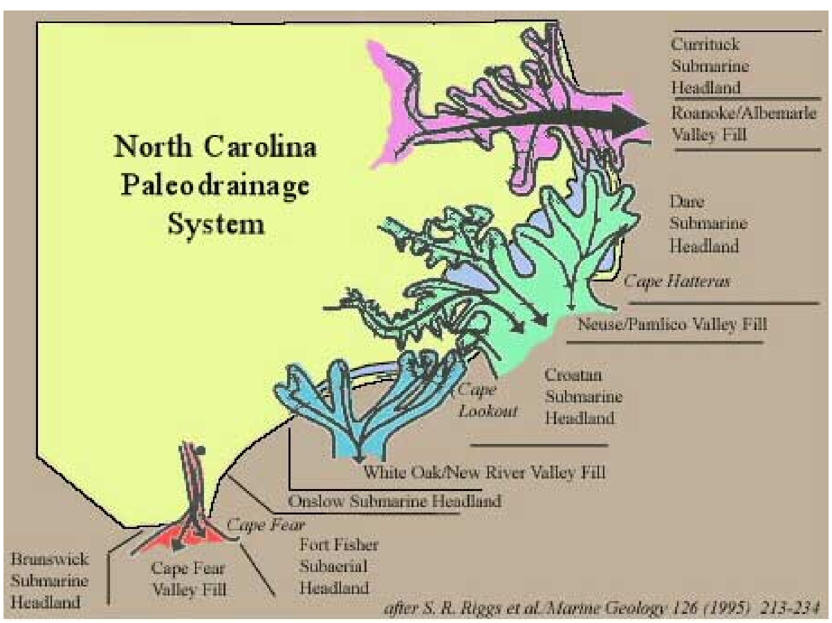


Figure 2. North Carolina's coastal paleodrainage system (from Riggs et al. , 1995). Of specific interest to this report is the ancestral Roanoke/Albemarle drainage system

.

oscillations across the low relief coastal plain and continental shelf is an extraordinarily complex mosaic of juxtaposed shallow marine to transitional marine and fluvial deposits of varying ages (Riggs et al., 1992; Snyder, 1993).

Interpretation of these complex relationships using traditional field geological methods (e.g. coring, stratigraphic correlation) is extremely difficult because of the piecemeal nature of preservation and erosion of deposits from different depositional episodes (Riggs et al, 1992). However, integration of criss-crossing geophysical profiling data has greatly aided in developing a coherent explanation of the Quaternary stratigraphy of the Albemarle estuarine system (AES) and its associated offshore equivalents. Seismic reflection profiles provide continuous records of subsurface stratigraphic architecture that can be correlated and definitively tied to depositional geometries observed on crossing profiles, and these data can be mapped to reveal their spatial distribution (e.g. Boss and Hoffman, 1999a-d, 2000). In addition, mapped seismic stratigraphic boundaries can be used to determine the three-dimensional geometry and volume of depositional units (Boss and Hoffman, 1999a-d; 2000).

Preliminary results documenting the gross geologic framework and seafloor character within the study area were previously reported by Boss and Hoffman (1997), Hoffman (1998), and Boss et al. (1999). Boss and Hoffman (1997) provided a preliminary assessment of the sand resource potential of the study area based on cursory examination of the seismic reflection data used for the present report. Hoffman (1998) refined the results of Boss and Hoffman (1997) by better delineating potential sand resource areas based on preliminary analyses of cores obtained in 1996. Finally, Boss et al. (1999) interpreted side-scan sonar data from the study area in an attempt to classify and characterize the seafloor. Results of their analyses indicated that observed variability of the reflection characteristics of seafloor sediments was related to exposure of different stratigraphic units on the seafloor throughout the study area. Correlation of observed reflective properties of seafloor sediments with cores indicated that seafloor sediments within the study area ranged from shallow marine shelf sands to interbedded fluvial/marine sand/mud (perhaps tidally influenced) to estuarine mud. Thus, it appears that the geologic framework of the study area displays characteristics almost identical to those described onshore and within the Albemarle Estuarine System (Riggs et al., 1992; Snyder, 1993; Riggs, 1996).

## METHODS

The primary database used to develop the three-dimensional geologic framework for this study consisted of seismic reflection profiles and side-scan sonar records (Fig. 1) as well as 56 vibracores obtained by the NCGS in 1996. The methodology used to analyze each element of the database are described in detail below.

### Seismic Reflection Profile Interpretation and Analysis

Seismic reflection data were archived as paper scrolls printed at the time of acquisition and in digital format on CD-ROM. Paper copies of these data printed at the time of acquisition were of limited utility because their quality is greatly influenced by physical sea-state at the time of the research cruise and by the acquisition software processing parameters. However, digital records of these data (archived on CD-ROM) were reprocessed using specialized software to enhance signal-to-noise relations and thus provide more interpretable versions.

Seismic reflection data were collected to a maximum “depth” of either 100 or 120 milliseconds two-way travel time (the standard vertical axis on seismic reflection profiles) during the initial survey. Seismic reflection profiles from the study area were reprocessed and interpreted to a maximum “depth” of 60 milliseconds two-way travel time. This depth was chosen as a compromise providing sufficient depth to assess the geological architecture of the study area while also enabling relatively fine-scale resolution of individual sedimentary units. In addition, data below 60 ms were often significantly degraded due to attenuation of the outgoing seismic impulse and superposition of reflection “multiples” on weakly reflecting horizons. Thus, stratigraphic units beneath this level are too deep beneath the seafloor to be adequately resolved in three dimensions for this study.

Precise conversion of two-way travel time to true depth requires knowledge of the velocity of *p*-waves through both seawater and sedimentary deposits - parameters that typically are not available during a survey. Thus, figures showing “depth” to a particular reflecting horizon are presented in milliseconds two-way travel time, the parameter recorded during data acquisition.

For this study, estimates of the thickness of stratigraphic units were obtained by using a standard seawater *p*-wave velocity of 1500 m/sec and assuming uniform *p*-wave velocity through the sediment column of 1800m/sec. The estimate of *p*-wave velocity in sediment of 1800 m/sec was obtained from published values of typical unconsolidated, surficial marine sand (Dresser Atlas, 1982), and this value was adopted for this study. This value was chosen as a conservative estimate, since it is likely that *p*-wave velocities in the subsurface are greater than 1800 m/sec. Thus, estimates of sediment thickness reported herein are considered to be minimum estimates since velocities of seismic transmission greater than 1800 m/sec will result in thicker deposits. Table 1 shows how the thickness in meters of a 20 ms seismic unit would vary through a range of *p*-wave velocity.

Seismic reflection profiles were interpreted using an iterative correlation method whereby prominent seismic reflectors were identified and correlated among closely spaced seismic profiles. An attempt was then made to extend these initial correlations throughout the entire surveyed area, cross-referencing and checking for appropriate “ties” frequently until the entire data set was interpreted. This process constituted the first iteration through the data.

Table 1. Example calculations showing the dependence of estimated deposit thickness on *p*-wave velocity. Example assumes a stratigraphic unit with measured “thickness” 0.020 seconds (20 ms) two-way travel time on a seismic reflection profile. For this study, a conservative *p*-wave velocity of 1800 m/sec was assumed. The equation relating p-wave velocity, two-way travel time, and thickness is: $(t_2/2) \times v_p = z$ where $t_2$ = two-way travel time (milliseconds), $v_p$ = *p*-wave velocity (in m/sec), $z$ = thickness (in meters).

| Two-Way Travel Thickness (seconds) | p-Wave Velocity (m/sec) | Thickness (m) |
|---|---|---|
| 0.020 | 1500 | 15 |
| 0.020 | 1800 | 18 |
| 0.020 | 2100 | 21 |

Following this step, all profiles were reviewed, and refinements to the initial interpretations made. This process constituted the second iteration through the data. The third iteration through the seismic data involved tabulating the geographic locations and depths of principal seismic reflectors for each time-event mark (approximately every 500 seismic shot points) and line crossing. These data were compiled in a spreadsheet and checked for consistency; the position and depth of a reflector should be the same on crossing seismic profiles. Anomalous reflector depth pairs were noted, and the associated interpreted seismic profiles checked again for accuracy.

Finally, the digitized locations of seismic reflectors were updated using spreadsheet software and the results exported to Geographic Information System (GIS) software. Once entered into the GIS, maps of depth to reflector surfaces (equivalent to structure contours) and stratigraphic unit thickness (equivalent to isopach maps) throughout the study area were generated providing the three-dimensional stratigraphic framework of this portion of the North Carolina continental shelf.

For this report, an attempt was made to correlate the principal reflectors identified within the offshore study area with several previous works describing the geologic framework of the barrier island and back barrier systems (Eames, 1983; Riggs et al., 1992). In addition, mapped seismic units were assigned preliminary age designations based on these correlations and previously developed chronostratigraphic divisions derived from amino acid racemization analyses of subfossil and fossil mollusk assemblages (York, 1984; York et al., 1989; Riggs et al., 1992). However, it should be noted that these interpretations are preliminary and based on extrapolation of stratigraphic relations from back barrier environments across the continental shelf, without any direct tying geophysical data. Thus, conclusions based on the suggested correlations should be viewed with great caution until better data become available.

### Side-Scan Sonar Interpretation and Analysis

All side-scan sonar records used for this study were obtained during the initial survey of the area and were acquired simultaneously with seismic reflection data. Original analog sonograms were available for review and interpretation, but data relating to specific operating parameters of the side-scan sonar instrument during acquisition were not available. Thus, it was not possible to determine whether slight changes in acoustic character of the seafloor were related to actual variability of seafloor physical properties or adjustment of operating parameters (such as gain) at the time of acquisition. As such, it was necessary to establish qualitative criteria for categorizing seafloor types. The side-scan sonar data were originally interpreted and analyzed by Boss et al. (1999) as part of an assessment of the sand resource potential of the study area.

All sonograms were recorded with a 400-m swath, though in some instances shallow water limited the effective imaging area on the seafloor to less than 400 meters. Time-event marks on the sonograms were cross-referenced to known navigation fixes associated with normal-incidence seismic reflection data and the GIS base map. Surface sediment in cores corresponding to characteristic acoustic textures observed on sonograms were examined in order to provide “ground truth” for interpretations of side-scan sonar data.

## Vibracore Analyses

The study area includes a total of 56 vibracores. These were taken during the summer of 1996 aboard the *R/V Seaward Explorer*. Core lengths ranged from 2.32 m to 6.07 m, with an average length of 4.94 m. Fig 1 shows the distribution of the core locations within the study. Appendix 1 contains information for individual cores and Appendix 2 contains histograms showing grain size distribution for whole core averages.

The project cores were cut into approximately 1 m lengths after being shipped to the Coastal Plain Office (CPO) of the NCGS in Raleigh, NC. At the CPO, 1-m core sections were split lengthwise and one half of the core was used for sampling while the other half was preserved for archival purposes. Core processing included visual description and logging, subsamples of sediment, and digital imaging via an 8 mm camcorder connected to an image capture device and a computer. Core images were archived on CD-ROMs and textural analyses (standard textural parameters such as weight percent size fractions, mean grain size, sorting, etc.) were compiled in computer spreadsheets. All core data were archived at the CPO.

Two-hundred eighty-eight subsamples of sediment were taken and analyzed for grain size distribution following methodology given in Folk (1964). Mud sand and gravel are size terms used to characterize the texture (grain size) of the cores. Mud refers to grains with a diameter less (finer) than 4 Ø (0.0625 mm), where Ø = $-\log_2$ of grain diameter in millimeters (Pettijohn, 1975). Sand-sized grains range from 4 Ø to –1 Ø (2 mm) and gravel is material coarser than –1 Ø (2mm). No pipette analysis was done on the mud fraction.

## SEISMIC REFLECTION RESULTS

Results of analyses of interpreted seismic reflection profiles are presented below as a series of maps showing measured depth (converted from two-way travel times) to principal reflecting horizons and as isopach maps of the thickness of stratigraphic units along with qualitative descriptions of the overall depositional geometry of each unit. A convention established by Boss and Hoffman (1999a-d, 2000) was used to designate the principal reflectors and associated stratigraphic units. The seafloor reflector was designated $R_0$, and each prominent reflector beneath the seafloor numbered sequentially throughout the study area (i.e. $R_1$, $R_2$, $R_3$, $R_4$). Since each seismic unit is bound by an upper and lower reflector, it was decided to label each stratigraphic unit according to its basal reflector. Therefore, the sedimentary unit bound by $R_0$ (upper) and $R_1$ (lower) is termed $S_1$, the unit between $R_1$ and $R_2$ is called $S_2$, etc.

Within the upper 60 ms of the seismic reflection profiles used for this study, six principal seismic reflectors were identified (designated $R_0$, $R_1$, $R_2$, $R_3$, $R_4$, $R_5$) and these reflectors subdivide the offshore stratigraphy into five mappable units (designated $S_1$ through $S_5$). Descriptions of each of these units are provided below. Thus, assuming superposition, seismic units are labeled in order of increasing age downward through the section.

### Seismic Unit $S_1$

Seismic Unit $S_1$ occupies the highest stratigraphic position within the study area and is bound by the present-day seafloor (reflector $R_0$) and the first-observed prominent reflector (reflector $R_1$). Seismic Unit $S_1$ occurs throughout the northern half of the study area. Its basal reflector ($R_1$) was observed to truncate a number of deeper parallel to sub-parallel reflectors (notably $R_2$ and $R_3$) throughout the northern half of the study area and was interpreted to be the deepest erosional surface developed within a complex series of nested fluvial channels that meander across the continental shelf (Fig. 3). Individual seismic reflection profiles in the northern portion of the study area are of excellent to good quality, and reveal remarkable detail of multiple channel incisions within unit $S_1$. However, the two nautical mile spacing of seismic profiles makes it impossible to map individual small channels across the shelf. Given the constraints of the present data set, it was only possible to indicate the lateral extent of channeled facies and present these lateral extents as boundaries on the accompanying map (Fig. 4).

In map view, it is evident that the spatial occurrence of reflector $R_1$ (and thus seismic unit $S_1$) defines a drainage network composed of several apparent stream subsystems joining a main system representing drainage from the Chesapeake Bay fluvial system to the northwest. The largest trunk channel appears to be that associated with the ancestral Albemarle River, which crosses the continental shelf west-to-east from Kitty Hawk Bay (Fig. 1). Several tributary systems join the paleo-Albemarle system (one from the west-northwest, one from the southwest) before the complex merges with the larger, east-southeast-trending drainage system near the seaward edge of the study area. It is also evident in map view that these fluvial systems must represent a complex of multiple channels that developed a broad fluvial plain during an interval of lower sea-level. The maximum width of the paleo-Albemarle system is greater than 7 nautical miles (13 km). This scale is more likely related to a broad flood plain rather than a single river channel.

The depth to reflector $R_1$ (Fig. 5) varies irregularly, but is generally deepest along the axis of channel systems. The minimum depth to $R_1$ was measured as approximately 20 m below sea-level in the nearshore region of the study area. Along the boundaries of the channel system, $R_1$ intersects the seafloor. The maximum depth to $R_1$ measured within the study area is approximately 50 m. Thus, the maximum observed relief within the channel system is on the order of 30 m. The channel system generally deepens eastward across the shelf. Comparing depth to $R_1$ with present-day bathymetry on the continental shelf indicates that $R_1$ might crop out on the seafloor just beyond the study area.

The map of the paleo-drainage systems (Fig. 4) is useful in establishing the extent of fluvial modification of continental shelf stratigraphy during sea-level lowstands. Note that virtually all of the northern portion of the study area falls within the boundaries of fluvial incision determined from seismic profile data, indicating the efficiency of fluvial processes to erode, rework, and cannibalize pre-existing stratigraphic successions during intervals of continental shelf emergence.

### Seismic Unit $S_2$

Seismic Unit $S_2$ was bound by the seafloor reflector ($R_0$) and reflector $R_2$. Reflector $R_2$ appeared to be a widespread reflecting horizon, occurring throughout the studied area. However, $R_2$ was truncated by channel incision related to formation of $R_1$ throughout the northern portion of the surveyed area, and only remnants of $R_2$ were mappable in interfluvial divides (Fig. 6). Thus, unit $S_2$ was completely removed by erosion where it was truncated by fluvial incision associated with development of unit $S_1$. Reflector $R_2$ displayed relatively low relief and sloped gently from the nearshore region of the study area to its offshore boundary; the slope of $R_2$ in the

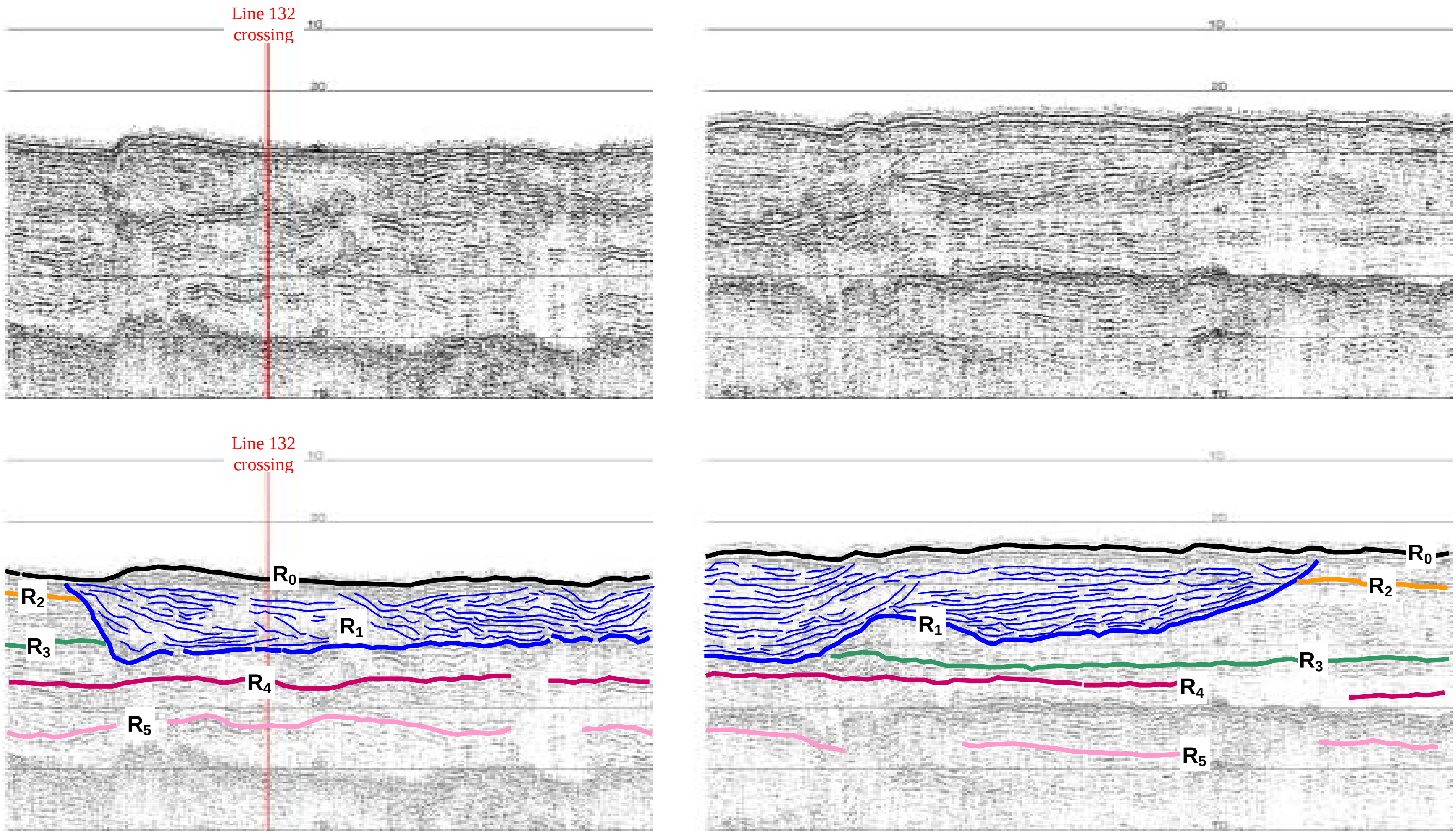


Fig. 3. Portion of seismic reflection profile 080 at intersection with line 132. Figure shows the north (left) and south (right) margins of the channeled seismic facies. Vertical scale is two-way travel time in 10 millisecond divisions (10 ms 2-way travel time is approximately 9 m). Total width of section is approximately 4.5 nautical miles (8 km). Upper image is processed, uninterpreted section. Lower is interpreted section showing channeled seismic facies and primary reflecting horizons $R_0$ – $R_5$.

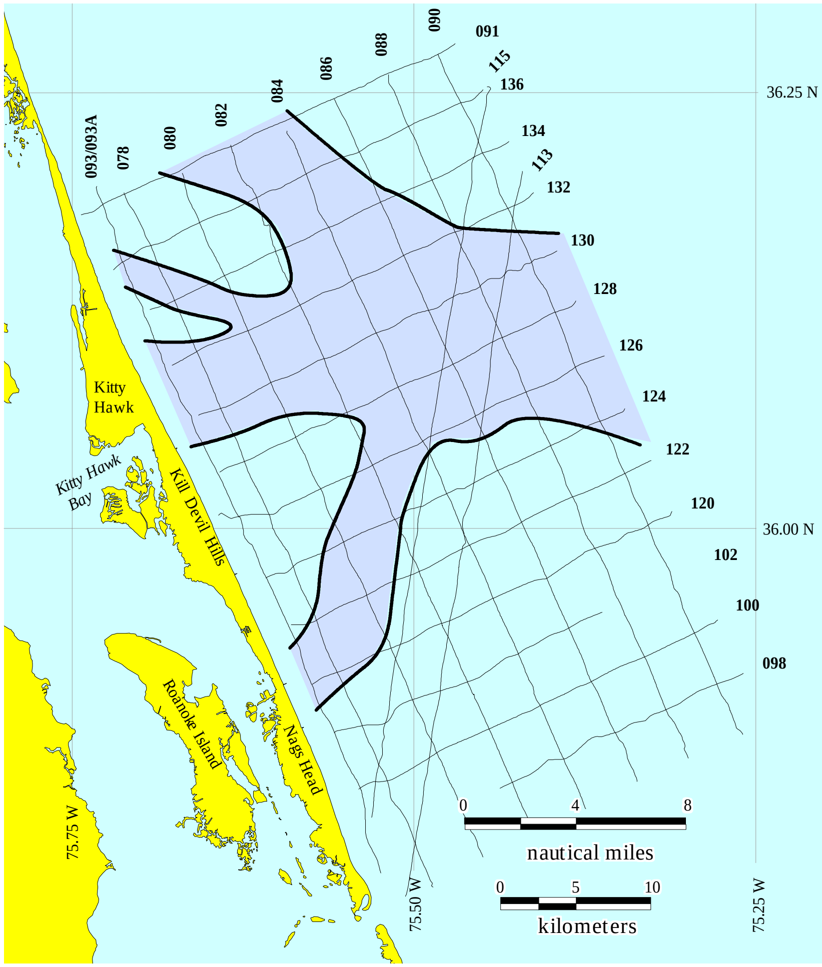


Figure 4. Outcrop/subcrop area of major paleofluvial valley system.

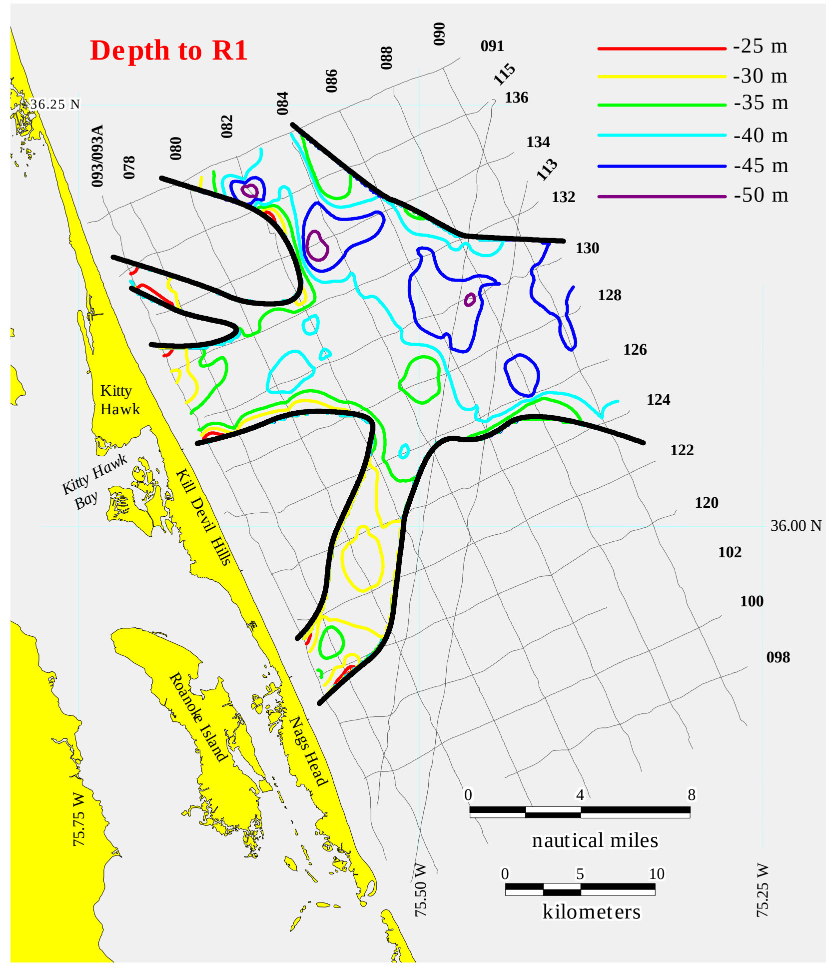


Figure 5. Structure contour map on reflector $R_1$.

offshore direction appeared to be approximately 1 m per nautical mile (approximately 0.03°) toward the east-southeast. The minimum observed depth to $R_2$ was 20 m below sea-level in the nearshore area and it slope uniformly to a depth of 40 m below sea-level in the southeastern portion of the study area.

The thickness of $S_2$ (Fig. 7) was determined by subtracting the depth of $R_2$ from $R_0$ throughout the study area. The maximum thickness of $S_2$ was 17 m and its average thickness was approximately 6 m. The unit is somewhat tabular in overall geometry and it was observed to thicken somewhat toward the east-southeast. Thickening of the unit was associated with the gentle downward ramping of reflector $R_2$ toward the east-southeast.

### Seismic Unit $S_3$

Seismic Unit $S_3$ was bound by reflectors $R_2$ (upper bound) and $R_3$ (lower bound). Reflector $R_3$ (Fig. 8) was a widespread reflecting horizon within the study area. However, $R_3$ was also truncated throughout much of the northern half of the study area by fluvial incision related to development of $R_1$. As was the case with $R_2$, $R_3$ was mappable only in interfluvial divides in the northern half of the study area. The occurrence of remnants of $R_3$ permitted reasonable mapping of this surface and also determination of the thickness of the overlying sedimentary unit, $S_3$.

The basal reflector of unit $S_3$, $R_3$, also displayed relatively low relief and sloped gently from the northwestern nearshore east-southeast toward the offshore boundary. The regional dip was very gentle toward the east-southeast with a gradient of approximately 0.75 m per nautical mile (approximately 0.02°). Reflector $R_3$ had a minimum depth of approximately 25 m below sea-level in the nearshore of the extreme northwestern portion of the study area. $R_3$ attained its maximum depth of approximately 45 m below sea-level in the southeast corner of the study area.

The thickness of $S_3$ (Fig. 9) was determined by subtracting the depth of $R_3$ from $R_2$ throughout the study area. The maximum thickness of $S_3$ was 22 m and its average thickness was approximately 8 m. The unit was tabular in overall geometry and it was observed to thicken somewhat toward the south. Thickening of the unit was associated with the gentle downward ramping of reflector $R_3$ toward the east-southeast.

### Seismic Unit $S_4$

Seismic Unit $S_4$ was bound by reflectors $R_3$ (upper bound) and $R_4$ (lower bound). Reflector $R_4$ (Fig. 10) was a widespread reflecting horizon within the study area. Unlike $R_2$ and $R_3$, however, $R_4$ was sufficiently deep that it was not truncated by fluvial incision related to development of $R_1$. Thus, the depth to $R_4$ and thickness of seismic unit $S_4$ are mappable throughout the entire study area.

Like the other basal reflectors within the study area, $R_4$ also displayed relatively low relief and sloped gently from the nearshore toward the east-southeast offshore boundary. The regional dip remained very gentle toward the east-southeast with a gradient of approximately 1 m per nautical mile (approximately 0.03°). Reflector $R_4$ had a minimum depth of approximately 30 m below sea-level in the nearshore of the extreme northwestern portion of the study area. $R_4$ attained its maximum depth of approximately 55 m below sea-level in the southeast corner of the study area. of $S_4$ was 21 m and its average thickness was approximately 8 m. The unit was tabular in overall geometry and it was observed to thicken somewhat toward the south. .

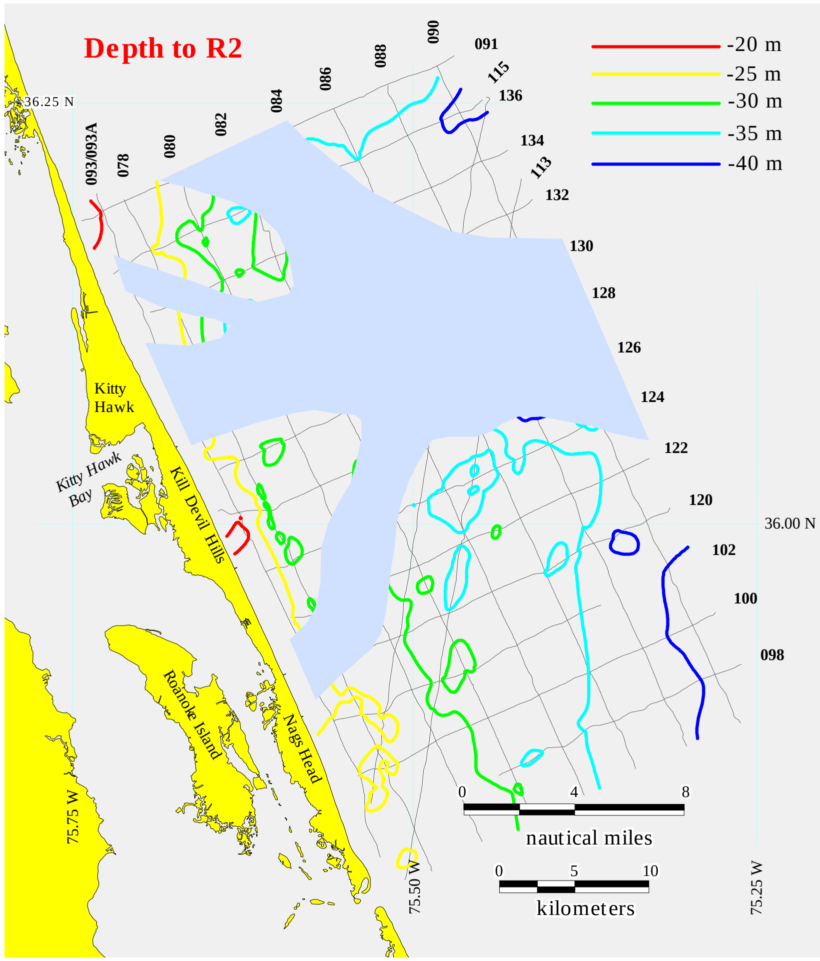


Figure 6. Structure contour map on reflector $R_2$. The channel system cuts through this reflector.

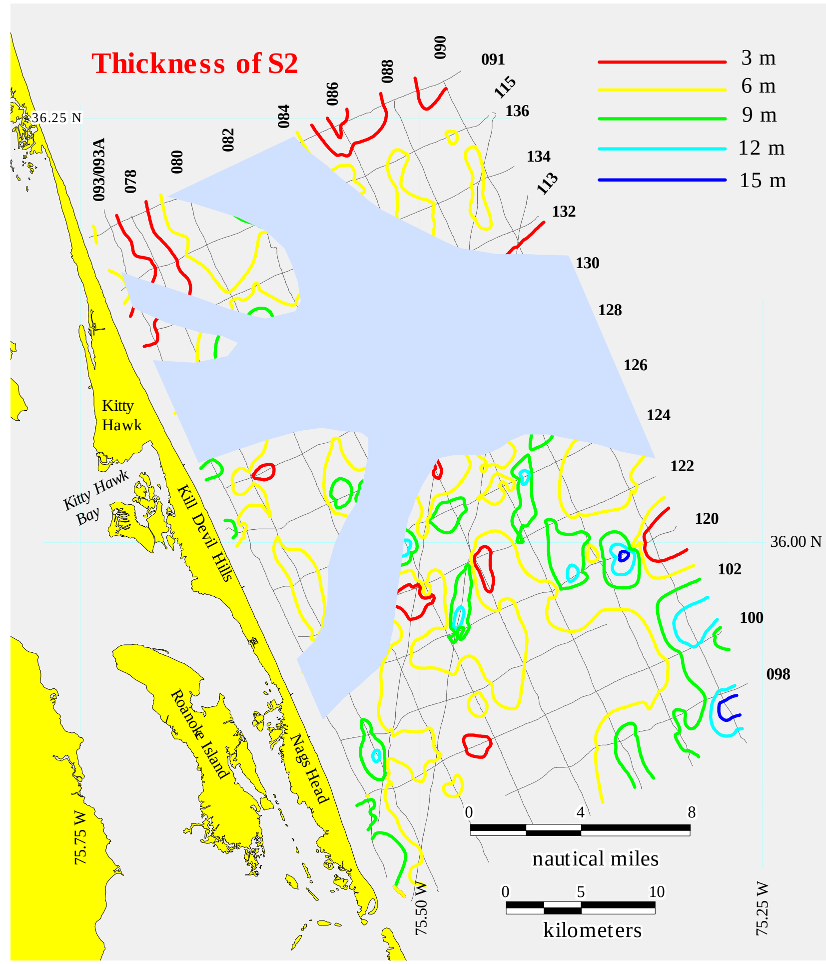


Figure 7. Isopach map of unit $S_2$. The channel system cuts through this unit.

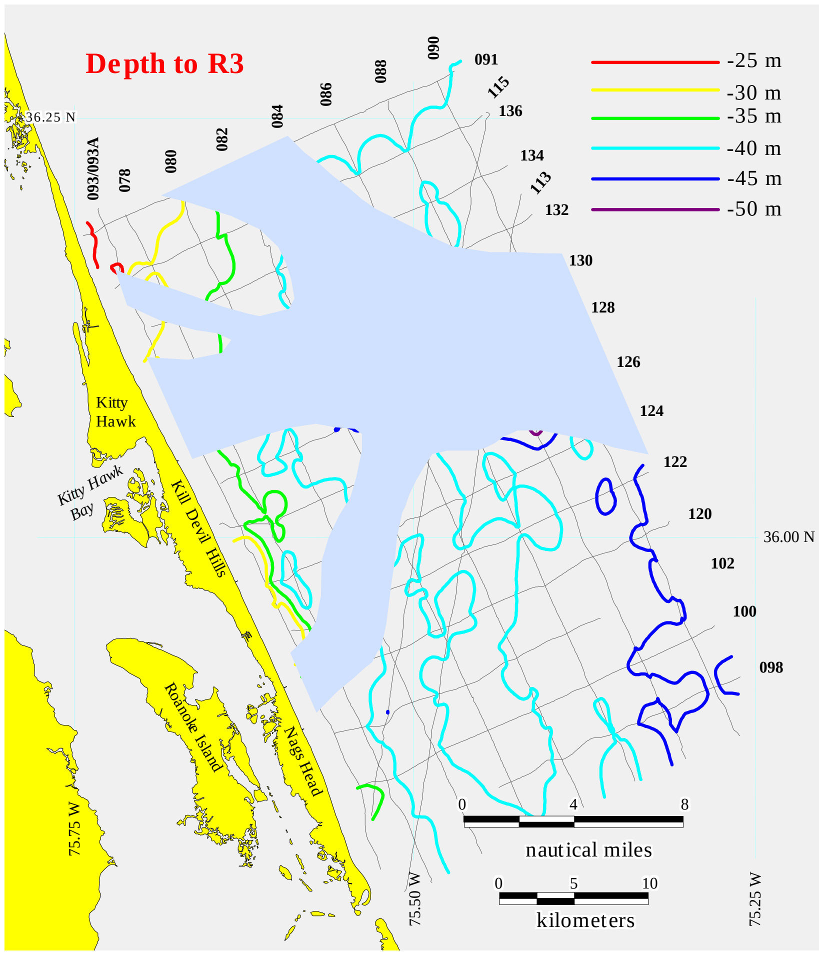


Figure 8. Structure contour map on reflector $R_3$. The channel system cuts through this reflector.

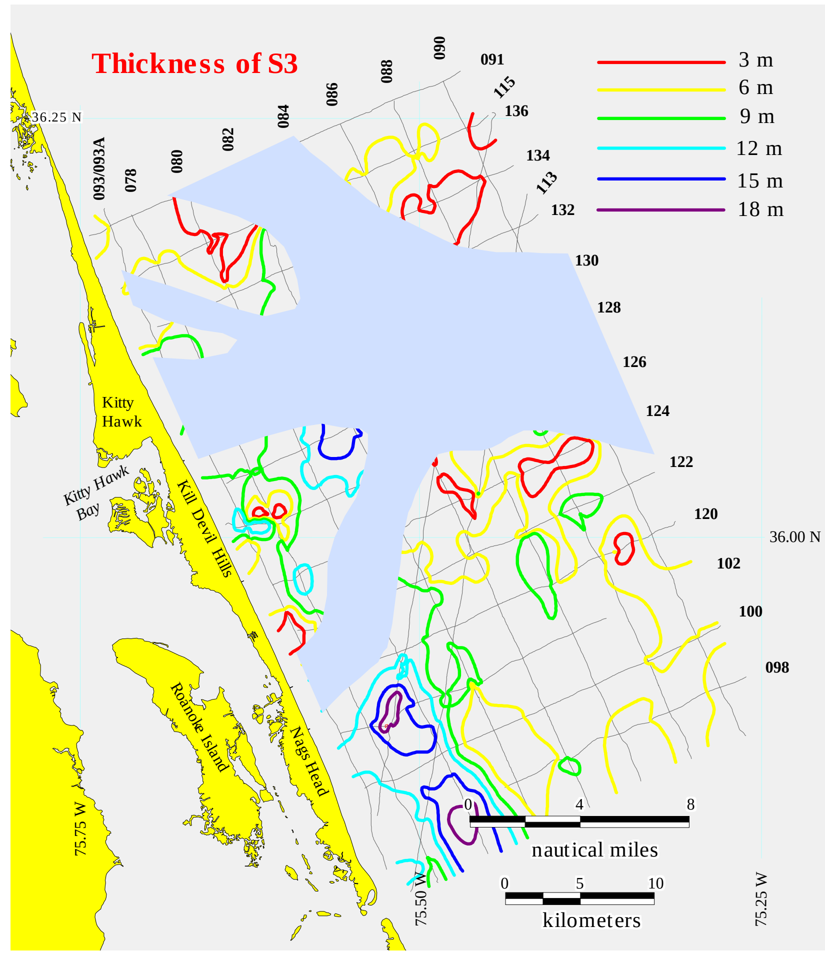


Figure 9. Isopach map of unit $S_3$. The channel system cuts through this unit.

Thickening of the unit was associated with the gentle downward ramping of reflector $R_4$ toward the east-southeast

The thickness of $S_4$ (Fig. 11) was determined by subtracting the depth of $R_4$ from $R_3$ throughout the study area. The maximum thickness of $S_4$ was 21 m and its average thickness was approximately 8 m. The unit was tabular in overall geometry and it was observed to thicken somewhat toward the south. Thickening of the unit was associated with the gentle downward ramping of reflector $R_4$ toward the east-southeast.

### Seismic Unit $S_5$

Seismic Unit $S_5$ was bound by reflectors $R_4$ (upper bound) and $R_5$ (lower bound). Reflector $R_5$ (Fig. 12) was interpreted to be a widespread reflecting horizon within the study area. However, identification of $R_5$ on seismic reflection profiles was discontinuous because the depth of the reflector beneath the seafloor caused it to frequently coincide with and be masked by “multiple” reflections from the seafloor reflector ($R_0$). Despite the discontinuous record of this reflecting horizon, it was identified in a sufficient number of locations to permit reasonable maps of this surface and its associated stratigraphic unit, $S_5$, to be generated within the GIS.

Like the other basal reflectors within the study area, $R_5$ also displayed relatively low relief and sloped gently from the nearshore toward the east-southeast offshore boundary. The regional dip remained very gentle toward the east-southeast with a gradient of approximately 0.75 m per nautical mile (approximately $0.02^{\circ}$). Reflector $R_5$ had a minimum depth of approximately 30 m below sea-level in the nearshore of the extreme northwestern portion of the study area. $R_5$ attained its maximum depth of approximately 70 m below sea-level in the southeast corner of the study area.

The thickness of $S_5$ (Fig. 13) was determined by subtracting the depth of $R_5$ from $R_4$ throughout the study area. The maximum thickness of $S_5$ was 23 m and its average thickness was approximately 9 m. The unit was tabular in overall geometry and it was observed to thicken somewhat toward the south. Thickening of the unit was associated with the gentle downward ramping of reflector $R_5$ toward the east-southeast.

## SIDE-SCAN SONAR RESULTS

Five seafloor types were defined by the acoustic character of the seafloor observed on analog side-scan sonar records: 1) a relatively weak acoustic return producing a generally uniform, featureless sonar record; 2) a moderate to strong acoustic return produced by seafloor sediments with stronger acoustic backscatter characteristics; 3) seafloor with mixed weak and strong acoustic backscatter producing a sonar record with a “patchwork” pattern of mixed light gray and medium- to dark-gray areas; 4) seafloor with overall weak acoustic backscatter but with small areas of stronger backscatter producing a characteristic “speckled” appearance on sonar records; 5) potential “hard-bottom” or “live-bottom” identified by the presence of small scarps evident on the side-scan sonar records (Boss et al., 1999). Detailed descriptions of these seafloor types follows. Their distribution was mapped along tracklines in the earlier report of Boss et al, 1999 through a portion of the MMS study area (Fig. 14).

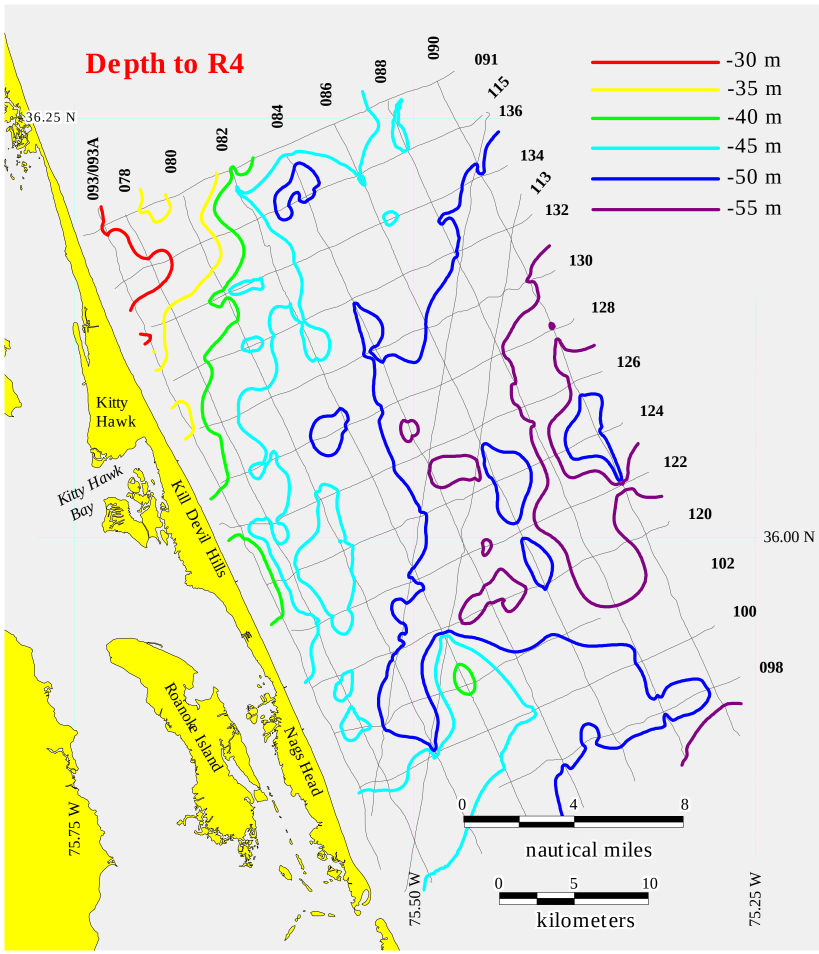


Figure 10. Structure contour map on reflector $R_4$.

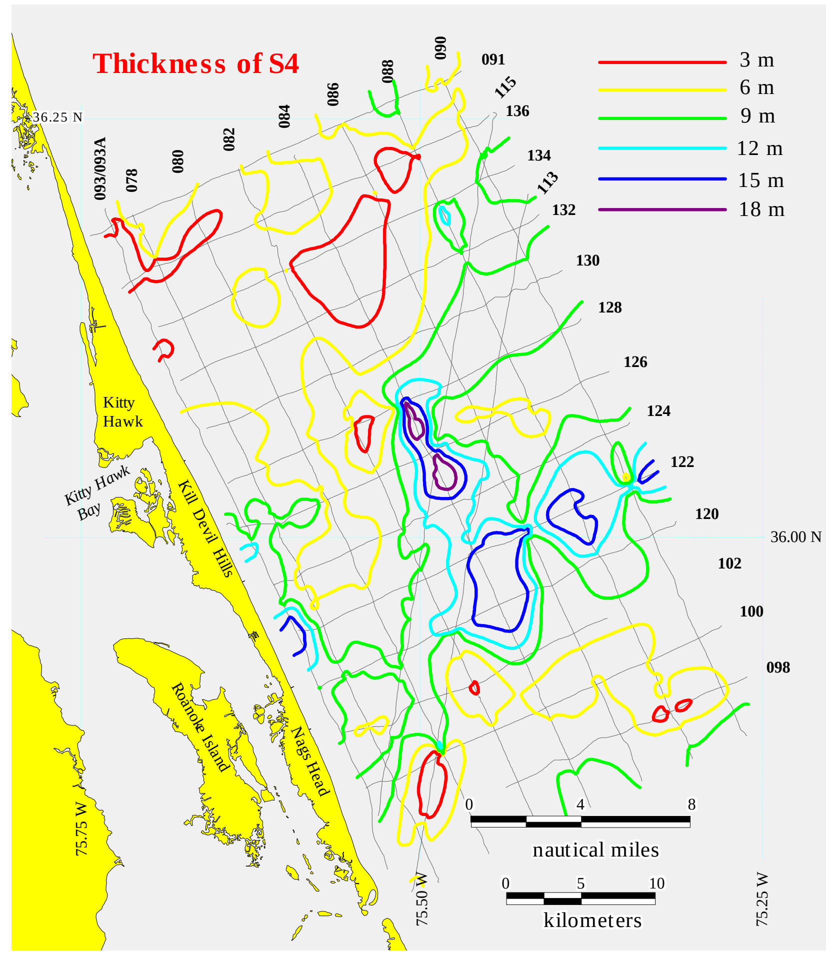


Figure 11. Isopach map of unit $S_4$.

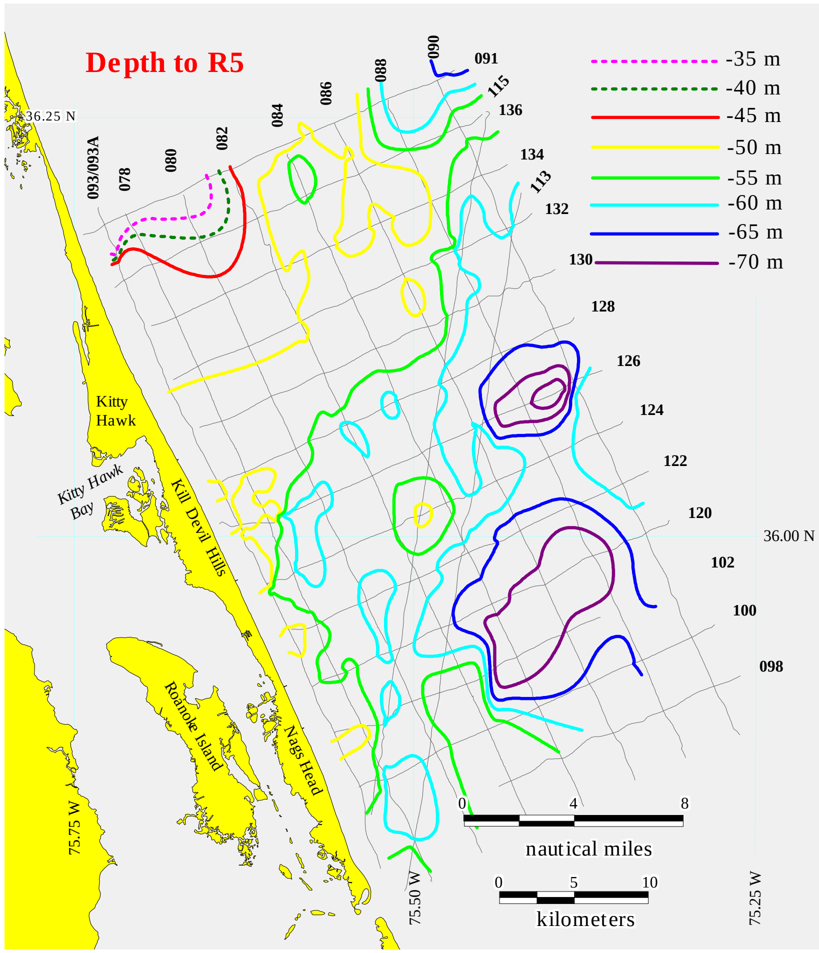


Figure 12. Structure contour map on reflector $R_5$.

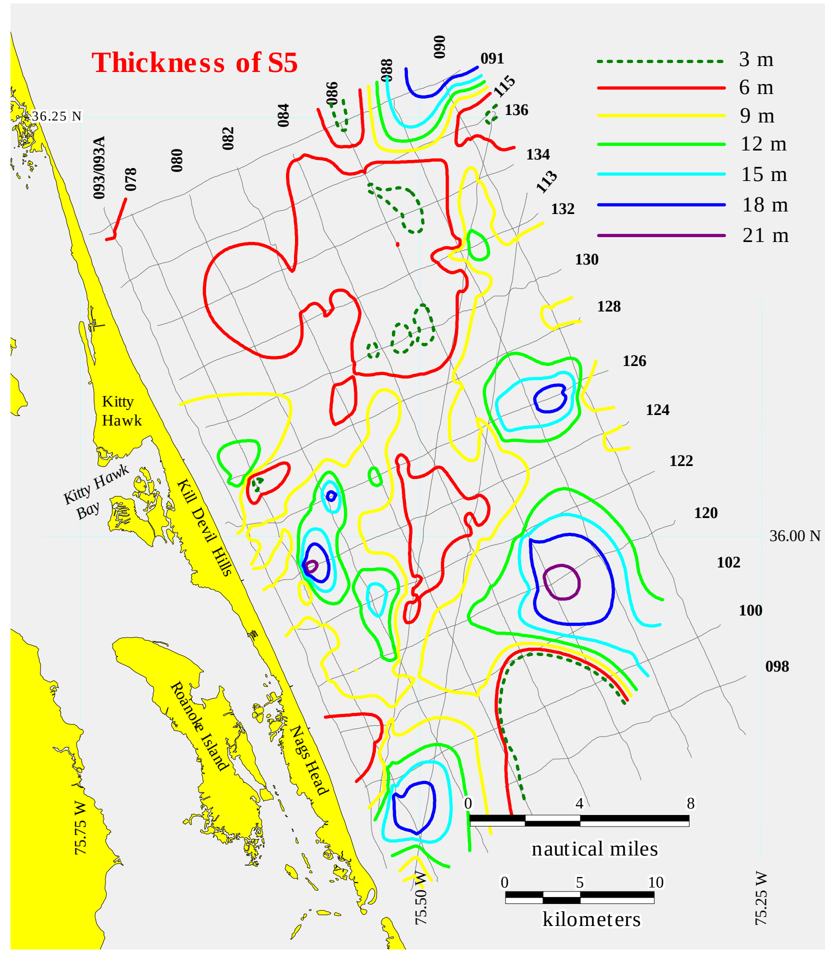


Figure 13. Isopach map of unit $S_5$.

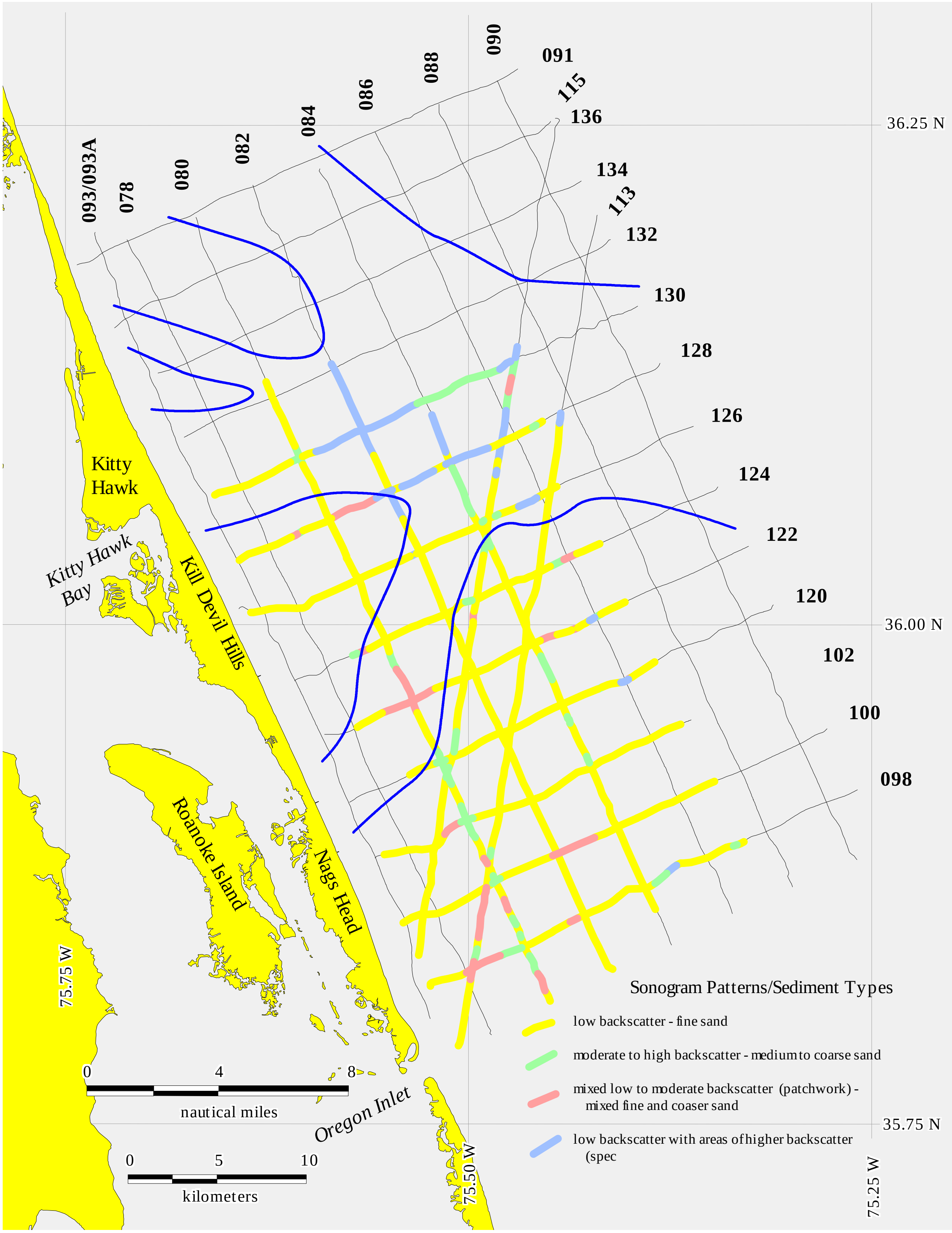


Figure 14. Distribution of the main side-scan sonar signatures seen in a portion of the study area (from Boss et al., 1999).

## Weak Acoustic Backscatter

The most commonly observed acoustic signature on side-scan sonograms was caused by relatively weak acoustic backscatter producing a uniform, featureless image (Fig. 15). Locally, ripple marks were occasionally visible on sonograms of this seafloor type. Similar side-scan signatures in Onslow Bay (central North Carolina shelf area) were shown by Riggs et al. (1998) to be characteristic of a mobile sand sheet.

Comparison of areas of this seafloor type to normal-incidence seismic profiles of the area indicates that it coincides with north-south trending bathymetric highs. The upper part of these highs typically is seismically transparent - suggesting relatively uniform sediment composition.

Textural analyses of sediment samples in cores through this seafloor type indicate that it is dominantly fine sand with relatively small quantities of mud and zones of medium to coarse quartz sand and shell gravel near its base (NCGS, unpublished data), suggesting a shallow marine depositional environment.

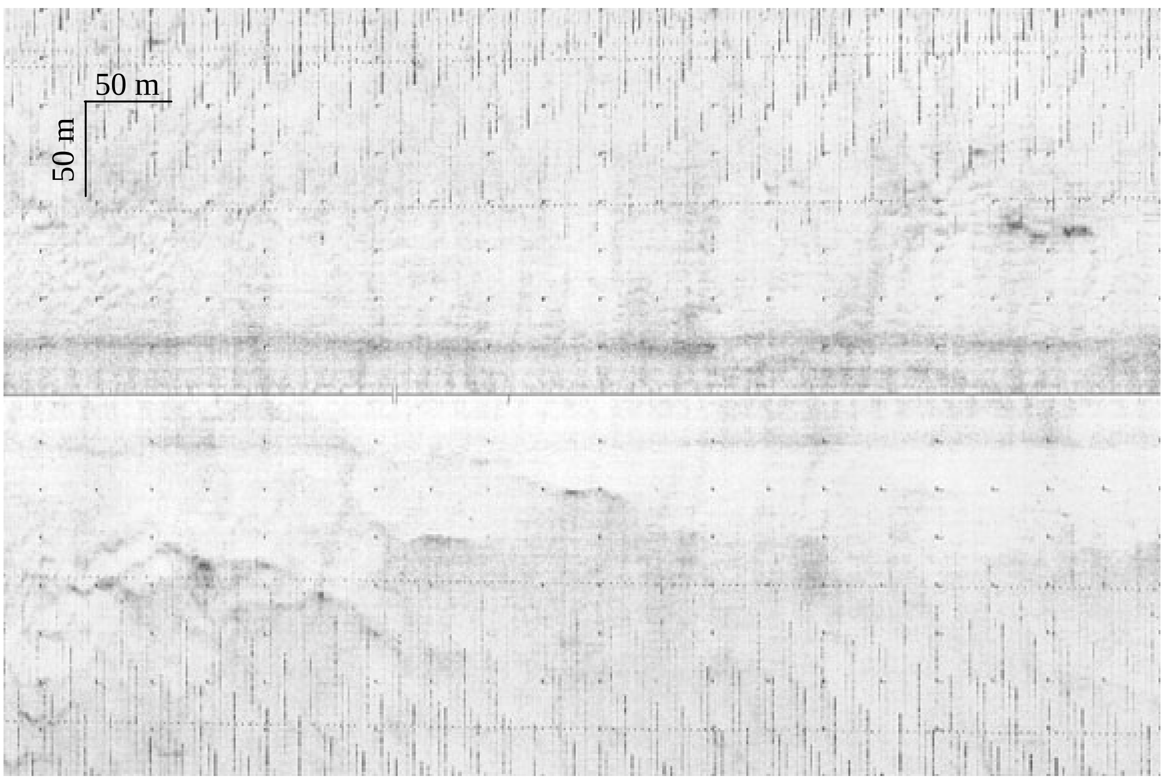


Figure 15. Example of weak acoustic backscatter (fine sand). Image is from line 128 approximately at core 012 just east of line 080 crossing. East is to the right.

## Moderate to Strong Acoustic Backscatter

Seafloor with moderate to strong acoustic backscatter produced a sonogram with medium to dark gray tone (Figs. 16) and was the second most common seafloor type within the study area. This signature was typically ripple-marked, with ripple crests spaced from 1 - 1.5 m. Comparison of areas displaying this seafloor type to normal-incidence seismic records indicated

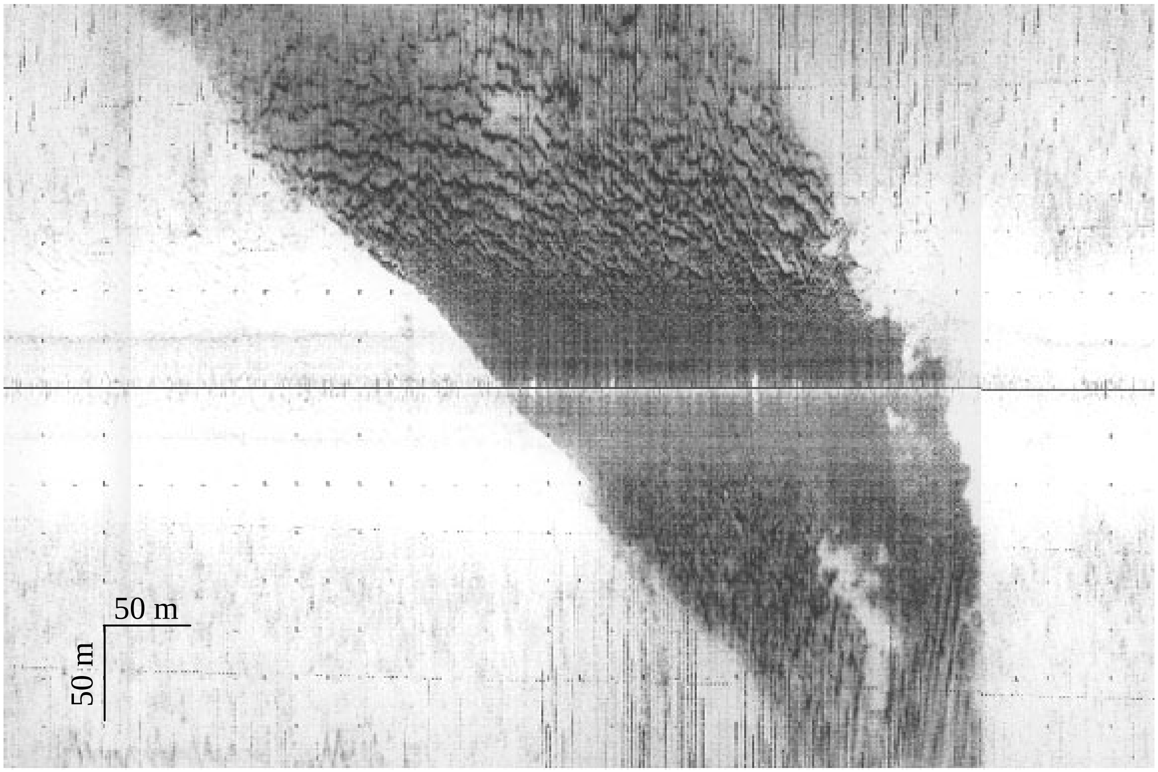


Figure 16. Example of moderate to strong acoustic backscatter sonogram signature (medium to coarse sand). Image is from line 080 just north of line 098 crossing. North is to the right.

that this seafloor type usually coincided with troughs located between the bathymetric highs of the southern part of the study area.

The stronger acoustic backscatter from this seafloor suggested that the sediment was coarser than that producing lower backscatter. Unfortunately, no vibracores were located where this acoustic signature was present. However, based on observed depth of this seafloor type in troughs, it is possible to extrapolate laterally on normal-incidence seismic sections to locations where vibracores penetrated sediments on bathymetric highs and apparently sampled sediment of this seafloor type near their base. Several cores penetrated the seismically transparent unit associated with the low backscatter sonogram signature. Medium to coarse sand (>30%) with gravel sized material (<15%) occurred in the basal part of these cores.

### Mixed Weak and Strong Acoustic Backscatter ("Patchwork" Seafloor)

The third seafloor type observed within the study area was characterized by alternating weak and moderately strong acoustic backscatter generating a characteristic "patchwork" pattern on sonograms (Fig. 17). Comparison of this seafloor type to seismic reflection records indicated that it was normally associated with slopes between bathymetric highs and lows. In fact, it was not unusual to observe the patchwork seafloor type grading upslope to uniform light gray (i.e. weak acoustic backscatter) and downslope to medium or dark gray (i.e. relatively strong acoustic backscatter) seafloor types.

This geometry suggested that the patchwork seafloor type resulted from fine sand transported downslope and partially covering coarser sediment exposed in troughs, or alternating fine and coarser grained lenses of a single stratum *in situ*. The vibracores within or proximal to this sonogram pattern did not provide definitive support for one interpretation over the other.

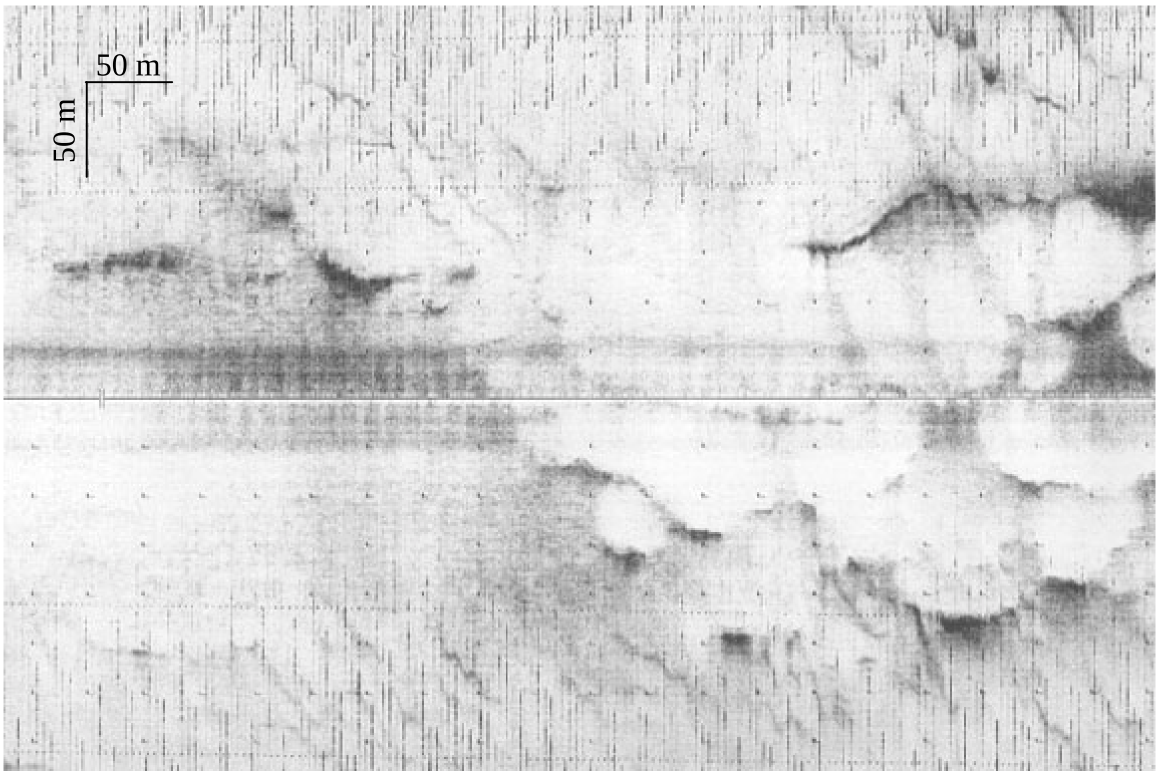


Figure 17. Example of moderately strong acoustic backscatter generating a characteristic "patchwork" sonogram signature. Image is from line 128 about midway between lines 080 and 082. East is to the right.

### Mixed Weak and Strong Acoustic Backscatter ("Speckled" Seafloor)

The fourth seafloor category recognized within the study area was characterized by relatively weak acoustic backscatter overall but with small linear to rounded areas (perhaps several $m^2$) of stronger backscatter producing a distinctive "speckled" appearance on sonograms (Fig. 18). This seafloor type was restricted to the northern half of the study area, and was predominantly over an area of relatively flat-lying seafloor at a depth typically >20m.

The occurrence of this seafloor type within the northern (deeper) sector of the study area suggested that it represented a stratum cropping out on the seafloor that was different than those observed to the south. Examination of seismic reflection profiles associated with the region where "speckled" seafloor occured suggested that this seafloor type was associated with sediments deposited within the boundaries of the paleofluvial system (Fig. 20).

Vibracores through "speckled" seafloor were dominantly mud with intercalated sand as laminae, lenses, and beds. This type of bedding suggested estuarine sediments that back-filled channels during episodes of sea-level rise. The "speckled" appearance of sonograms was interpreted to result from exposure of the intercalated sands (relatively high acoustic backscatter) among the dominantly muddy sediment (low acoustic backscatter) on the seafloor.

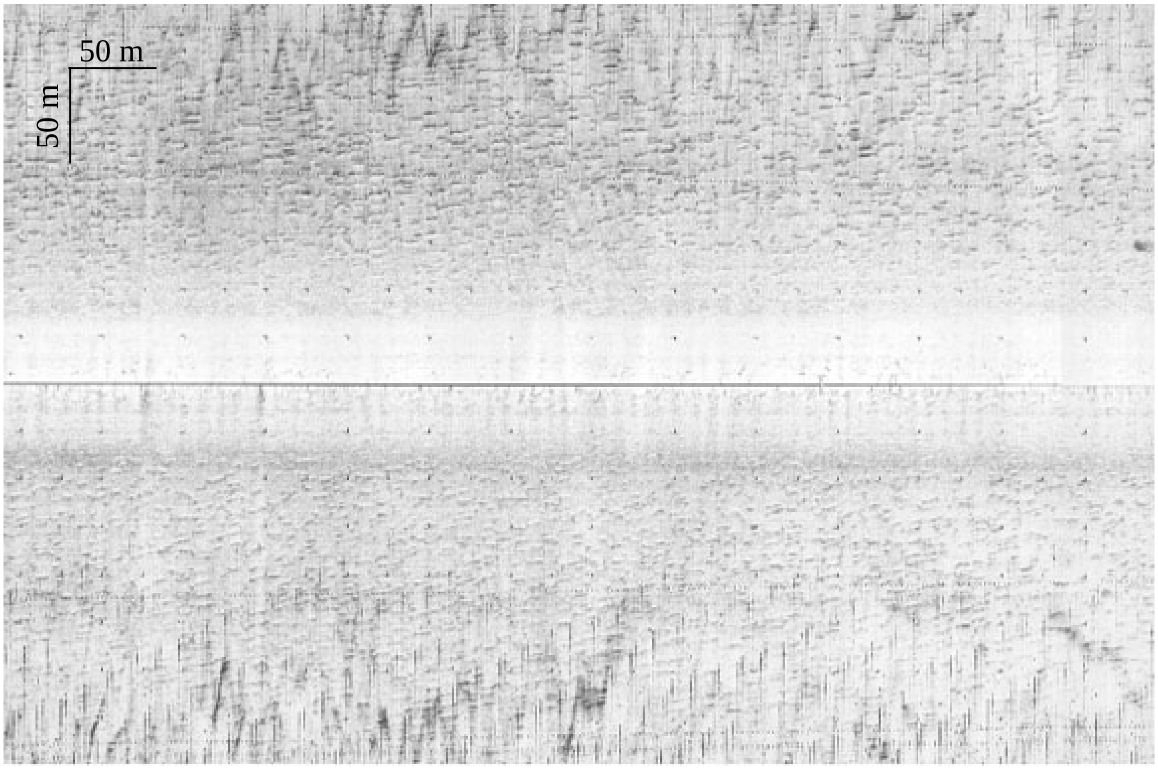


Figure 18. Example of relatively weak acoustic backscatter overall but with small linear to rounded areas (perhaps several m$^2$) of stronger backscatter producing a distinctive "speckled" appearance. Image is from line 130 just west of core 014A (a muddy core). East is to the right.

### Scarps

Hard-bottom may refer to any seafloor that is sufficiently indurated to stand out in relief against the surrounding seafloor. Riggs et al. (1996) provide a number of criteria for recognizing hard-bottoms from seismic and side-scan sonograms. Thus, recognition of hard-bottom siteswithin this study area depends on the expression of surface relief producing scarps or sloped ramps that were observed on both normal-incidence seismic and side-scan sonar profiles. Only a few vertical or near vertical features similar to hardbottom signatures reported from Onslow Bay (Riggs et al., 1998) were identified during this analysis and these sites are small (<0.5 km$^2$).

## VIBRACORE RESULTS

Using the *p*-wave velocity adopted for this study (1800 m/sec), the average core length would be represented on seismic profile data by 4.5 ms two-way travel time. Minimum and maximum length cores would penetrate to 1.5 ms to 5.5 ms two-way travel time on seismic profiles. Thus, it is clear that cores penetrate to very shallow depths within the sediment package.

The vibracores contain two major divisions of lithofacies: a sand dominated lithofacies (Type I) and a mud-dominated lithofacies (Type II). These can be further classified with Type I being divided into four subfacies and Type II being subdivided into two subfacies. Example images of each subfacies are contained in Fig 19. Water depth, core length, and various textural parameters are summarized in Table 2 below.

Type I subfacies include:

- IA clean, laminated to massive quartz sand that ranges from fine to medium grained;
- IB coarse sand to gravel that consists of both quartz grains and broken and weathered fossil fragments – this subfacies may be bounded by sharp erosional contacts at top and bottom;
- IC normally graded quartz sand fining upward from a fossil rich gravel locally to a silty clay cap – this subfacies may include local intervals of flaser bedding and muddy laminations;
- ID reverse graded quartz sand and gravel that is fossil rich at top.

Type II subfacies are:

- IIA interbedded clayey sand/silt to a silty/sandy clay that is laminated to lenticular bedded but may locally range from laminated to wavy or flaser bedded. Locally, the laminations may be chaotic or convoluted, and burrowed. This subfacies may include a granule size, fossil rich (*Mulinia*) gravel with the shells being inarticulate and ranging from fresh to weathered.
- IIB mud rich massive and bioturbated quartz sand, ranging from a fine to medium grained.

Table 2. Summary data for each major lithofacies type and for all cores. Mean Grain Size (GS) was determined statistically after (Folk, 1964). The mean GS (mm) is a conversion of the phi (Ø) value.

| | **Length (m)** | **$H_2O$ (m)** | **$H_2O$ (ft)** | **Mean GS (Ø)** | **Std. Dev. (Ø)** | **Mean GS (mm)** | **Wt. % Sand** | **Wt. % Mud** | **Wt. % Grv** |
|---|---|---|---|---|---|---|---|---|---|
| **Type I (n=32)** | | | | | | | | | |
| minimum | 2.32 | 16.84 | 51.00 | 1.26 | 0.60 | 0.14 | 57.90 | 1.20 | 0.01 |
| maximum | 6.07 | 30.71 | 93.00 | 2.84 | 1.38 | 0.42 | 98.12 | 38.41 | 15.56 |
| average | 4.93 | 24.38 | 73.81 | 2.33 | 0.92 | 0.21 | 84.88 | 11.17 | 3.74 |
| **Type II (n=24)** | | | | | | | | | |
| minimum | 1.71 | 20.15 | 61.00 | 2.55 | 0.55 | 0.06 | 28.84 | 21.99 | 0.01 |
| maximum | 6.06 | 32.69 | 99.00 | 4.05 | 1.72 | 0.17 | 77.17 | 70.74 | 13.83 |
| average | 5.13 | 26.08 | 78.96 | 3.30 | 0.97 | 0.11 | 55.05 | 42.13 | 2.56 |
| **ALL (n=56)** | | | | | | | | | |
| minimum | 1.71 | 16.84 | 51.00 | 1.26 | 0.55 | 0.06 | 28.84 | 1.20 | 0.01 |
| maximum | 6.07 | 32.69 | 99.00 | 4.05 | 1.72 | 0.42 | 98.12 | 70.74 | 15.56 |
| Average | 5.01 | 25.10 | 76.02 | 2.75 | 0.94 | 0.16 | 72.09 | 24.44 | 3.23 |

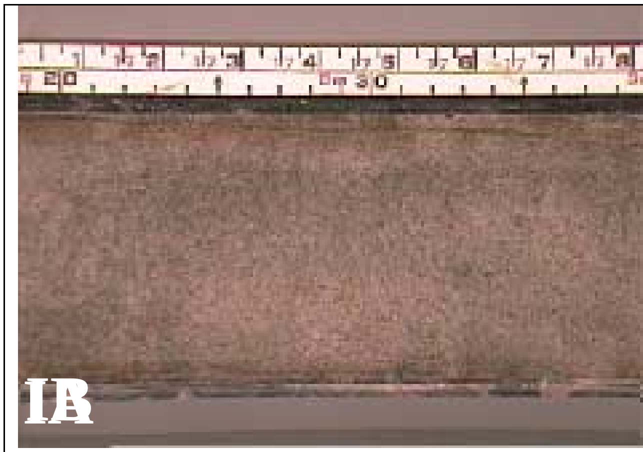

MMS-007 - 519 cm – 539 cm

MMS-001 - 340 cm – 358 cm

MMS-003 - 060 cm – 080 cm

MMS-003 - 170 cm – 189 cm

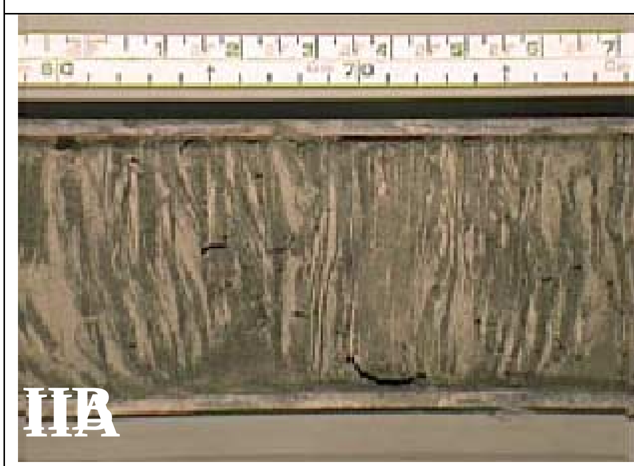

MMS-029 – 059 cm – 079 cm

MMS-011 - 020 cm – 039 cm

Figure 19.  Representative images of each of the six lithofacies identified in the vibracores.

Few cores are purely one single lithofacies subtype. Many contain a mixture of Type I and Type II lithofacies, so classification was a matter of determining the majority lithofacies type for each core. Thirty-seven of the 56 cores in the project area contain greater than 10 weight percent mud. The maximum mud content of any Type I core was 38 percent, and 7 Type I cores contained greater than 20 percent mud. A substantial number of Type I cores (12) contain greater than 10 weight percent mud, the amount of mud generally used as the threshold to determine acceptability for use as beach fill. No specific limit on mud content has been established, however, for offshore mining in Dare County.

As would be expected, the average grain size of Type II cores was considerably finer (3.30Ø = 0.11 mm or very fine sand) than Type I cores (2.33Ø = 0.21 mm or fine sand). When cores were sorted by weight percent mud, Type II cores make up 23 of the 26 muddiest cores.

Figure 20 shows the distribution of cores coded by major lithofacies type and by mud content greater than or less than 10 weight percent mud. The relation between paleofluvial channels, high mud content, and Type II cores, became apparent when core locations were plotted on seafloor maps. Only a single Type II core (052) is located south of the paleofluvial channel area. On the other hand, numerous Type I cores occur within and to the north of the channel area. However, most Type I cores occurring within the channeled area were located on bathymetrically high areas that post-date the channel infill (for example, cores 009, 010, 011, 013, 042, 044, 032, and 034).

The inference drawn from the distribution of lithofacies was that: 1) the Pleistocene platform area was comprised of mixed sediment types, 2) the paleofluvial valley fill was mud-prone, and the bathymetrically high areas (shoals) were sand-prone. Lithofacies Type IA would be the best quality sand for beach fill material because of its low mud content. Its common occurrence on bathymetrically high areas suggests that these bodies would be the areas of greatest potential to host sand resources for beach nourishment.

## DISCUSSION

Results of this study clearly document the occurrence of a large paleofluvial system crossing the continental shelf (Fig. 21) in the northern half of the study area. This fluvial system was undoubtedly established during an episode (or episodes) of lowered sea-level when the continental shelf was emergent. The primary east-west trunk of the fluvial system corresponds to the ancestral Albemarle River drainage (Riggs, 1996; Snyder, 1993; Riggs et al., 1992; Eames, 1983) and matches the trace of this drainage documented from studies of the back barrier estuarine system (Riggs, 1996; Riggs et al., 1992) and core borings on the island (Eames, 1983). Thus, results of this study extend the known trend of this paleo-drainage pattern offshore toward the shelf edge.

It is also clear from the results of this study that the paleo-Albemarle fluvial system was responsible for extensive erosion, reworking, and re-deposition when the shelf was exposed. Downcutting of the river and lateral migration or meandering of the main channel appears to have efficiently removed shelf stratigraphic units to a maximum depth of at least 50 m beneath present-day sea-level. The area of the flood plain associated with the drainage system was estimated from the GIS to be at least 473 $km^2$ (approximately 35% of the study area). Seismic

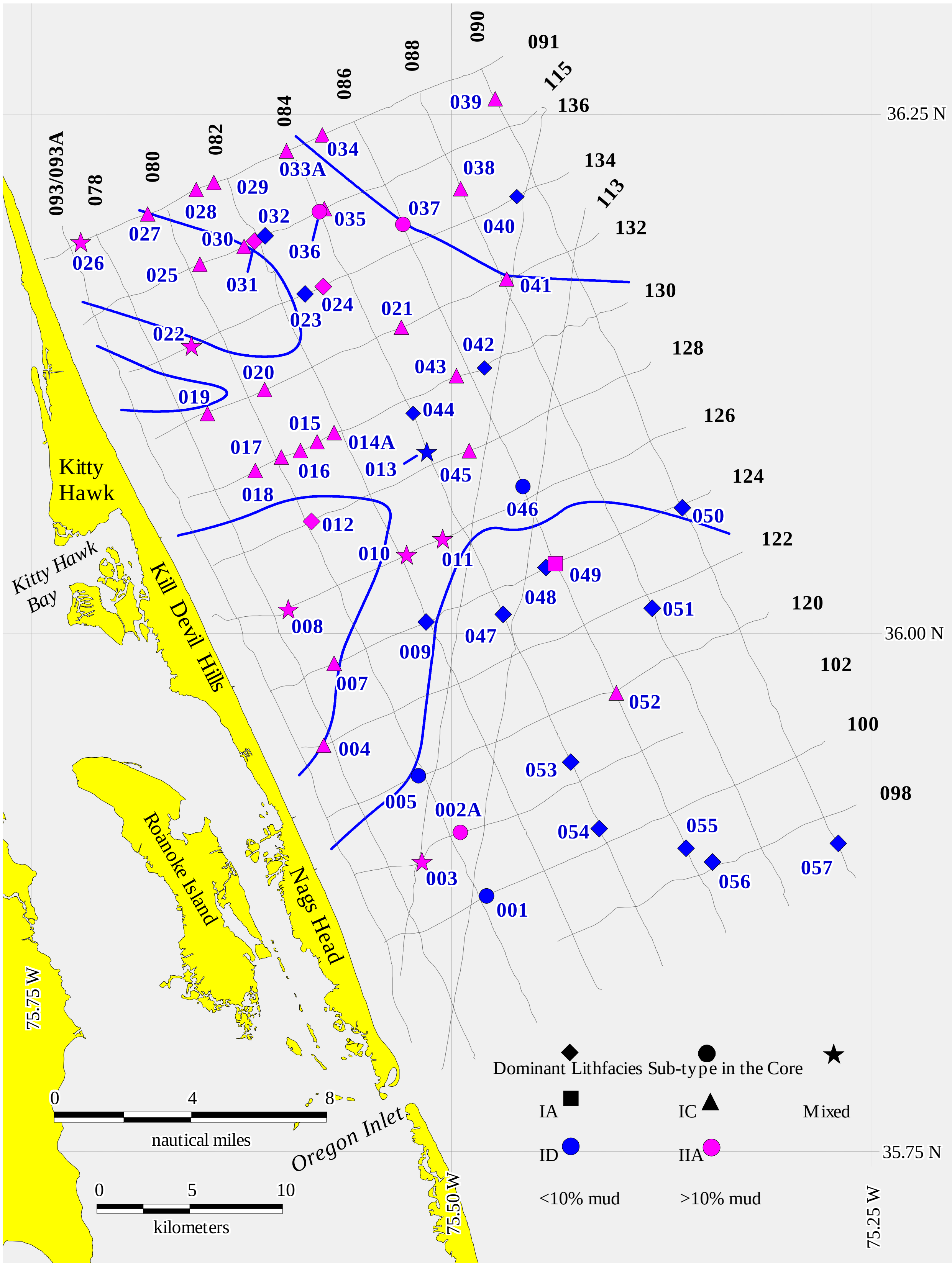


Figure 20. Distribution of cores by dominant lithofacies type for the entire core ("mixed" where no type is dominant) and by weight percent mud in entire core.

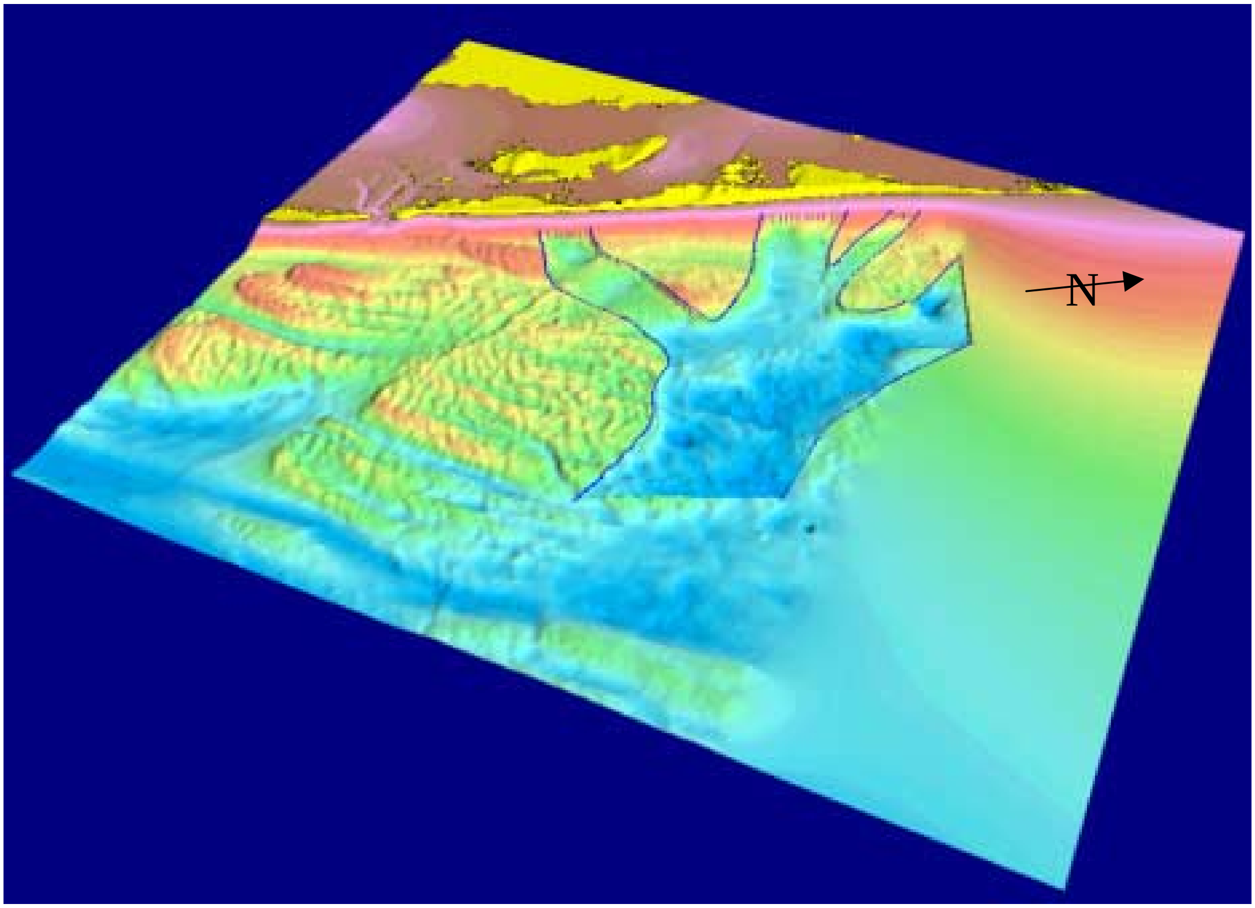


Figure 21. Perspective view (azimuth = 70° , elevation = 45°) of the inner shelf off northern Dare County. The surface is of present bathymetry with unit $S_1$, the channel fill sequences, removed. Thus, this might approximate the pre-Holocene surface.

units $S_2$ and $S_3$ were completely removed by erosion as the fluvial system evolved, and only remnants of these units can be found in interfluvial divides (Figs. 6–10).

The sedimentary succession filling the paleofluvial system correlates with Depositional Sequence 7 (DS-7) of Riggs et al. (1992) and Depositional Sequence V of Eames (1983), which was determined by those authors to be early to mid-Holocene. However, it is obvious that development and evolution of the paleofluvial system pre-dates its backfilling with estuarine deposits. The great areal extent of paleofluvial features observed on seismic reflection data suggests that this system was actively evolving on the continental shelf over a relatively prolonged interval. The basal reflector of the ancestral Albemarle fluvial system identified in this study (reflector $R_1$) was incised into Despositional Sequence 6 (DS-6) of Riggs et al. (1992) and DS-IV of Eames (1983).

Amino acid racemization assays of shells from DS-6 yield leucine-isoleucine ratios equivalent to Amino Zone 1 of York et al. (1989) with an estimated age between 78 – 51 ka. Thus, DS-6 appears to have been deposited in part near the termination of oxygen isotope stage 5 (possibly stage 5a). Given that reflector $R_1$ post-dates deposition of DS-6, it would appear that the timing of incision of the fluvial system across the continental shelf is constrained by this date and the post-glacial transgression that began approximately 18 ka (Fairbanks, 1989). Furthermore, the maximum depth of incision below present sea-level was observed to be at least 50 m (Fig. 6), requiring a base level change of at least that magnitude. As such, it appears that the age of the paleo-Albemarle system must correspond to the Wisconsin Age glaciation and sea-level lowstands (oxygen isotope stages 4, 3, 2; Dawson, 1992). The North Carolina continental shelf would have been fully exposed throughout this glacial stage where sea-level lowering ranged from 30 m to 125 m (Bloom et al., 1974, Chappell 1974; Chappell, 1983; Shackleton, 1987).

Following the reasoning above and applying the Principles of Cross-Cutting Relationships and Superposition, sedimentary deposits truncated by or below reflector $R_1$ must be older. An attempt to determine how much older relied on tentative correlation of offshore seismic units with depositional sequences identified from cores through the modern barrier island (Eames, 1983; Riggs et al., 1992). The observed depth to the base of Seismic Unit $S_2$ in the nearshore region is approximately 25m below sea-level (Fig. 7). This seems to correspond to the base of Depositional Sequence 6 (DS-6) of Riggs et al. (1992). Thus, sediments of Seismic Unit $S_2$ are correlative with sediments of DS-6, which has an estimated age falling within Amino Zone 1 (78 – 51 ka; York et al., 1989).

The basal reflector of Seismic Unit $S_3$ had an estimated depth in the nearshore zone of the study area of approximately 30 m below sea-level. Correlation of this unit with depositional sequences of Riggs et al. (1992) was difficult because of the absence of a direct stratigraphic tie or other constraining information. However, extrapolation of apparent regional dip from Riggs et al. (1992) figure 2 suggests that Seismic Unit $S_3$ could be equivalent to Riggs et al. (1992) DS-3. DS-3 was determined by Riggs et al. (1992) to fall within Amino Zone 3 (York et al., 1989) with an estimated age range between 530 – 330 ka. This correlation should be considered very tentative, however.

Seismic Unit $S_4$ has a basal reflector ($R_4$) with estimated depth of 40 m below sea-level in the nearshore region of the study area. This depth is greater than that represented by Riggs et al. (1992) on their figure 2, so correlation of this unit to previously identified units is highly speculative. The estimated depth to the base of this unit was determined by applying a uniform, average *p*-wave velocity of 1800 m $s^{-1}$ to measured two-way travel time to derive depth. Variation in this parameter, especially toward slightly lower velocities, would change the position of this reflector to shallower depths that might lead to better correlation. Alternatively, this reflector may be at greater depth than onshore boundaries due to regional dip in the offshore direction. At any rate, reflector $R_4$ and its associated stratigraphic unit, $S_4$, may correspond to DS-2 of Riggs et al. (1992). If so, $S_4$ would fall within Amino Zone 1 of York et al. (1989), with an estimated age range of 1.8 – 1.1 Ma. This correlation would place $S_4$ in the early Quaternary.

Seismic Unit $S_5$ has a basal reflector ($R_5$) with estimated depth of 50 m below sea-level. This places $R_5$ in proximity to a reflecting horizon interpreted to be the Pliocene-Pleistocene contact by Riggs et al. (1992; Figs. 9, 10). Assuming that the age assignment of the overlying seismic unit is correct, placement of the Pliocene-Pleistocene boundary at $R_5$ would be reasonable.

Results of this study indicate that the geologic framework of the continental shelf offshore Oregon Inlet to Kitty Hawk, North Carolina is composed of a succession of tabular stratigraphic units dipping at very slight inclination toward the east-southeast. The two uppermost stratigraphic units ($S_2$ and $S_3$) were truncated by incision of a fluvial system during an interval of lowered sea-level that allowed rivers to establish channels across the northern portion of the study area. The timing of fluvial incision seems to be reasonably constrained by cross-cutting and superpositional relationships with dated strata known from onshore sections (Eames, 1983; York et al., 1989; Riggs et al., 1992) and would have to have occurred during oxygen isotope stages 4, 3, and 2 (Wisconsin Age; Dawson, 1992).

Correlation of seismic unit $S_2$ (this study) with DS-6 (Riggs et al., 1992) is also constrained by these relationships. Other correlations are more tentative, but it appears from stratigraphic relations that seismic units $S_3$ – $S_5$ should all be placed in the Quaternary Period, with the Pliocene-Pleistocene epochal boundary coinciding with the basal seismic reflector of $S_5$ (i.e. $R_5$). Confirmation of these tentative correlations will require additional data, especially from deep bore holes through the modern barrier island system and insular continental shelf.

## SAND RESOURCES

Dare County has an ongoing federal beach nourishment project, the Northern Dare project. As of February, 2001, the feasibility portion of this project was being completed and the planning, engineering, and design phase was beginning. The project includes two primary areas of nourishment sites: a southern project area that is about 8.7 miles long located within Nags Head, and a northern project area that is about 3.8 miles long located in northern Kill Devil Hills and southern Kitty Hawk. Proposed borrow sites for the project's sand have been identified off of each project area. Initial construction was scheduled to begin in 2004 with a 3-year construction period and then annual maintenance each year after that for a project life of 50 years (project info from U.S. Army COE, Wilmington District, personal communication).

Figure 22 shows the proposed fill and borrow sites. The COE estimates sand volume of the $S_1$ site at 104.5 million cubic yards, the $N_1$ site at 5.2 million cubic yards, and the $N_2$ site at 2.4 million cubic yards. Area $S_1$ lies on a large shoal feature (part of Platt Shoals) which extends into federal waters

The proposed borrow area, however, is limited to within state waters (inside 3 nautical miles). Both of the northern borrow areas appear to be located along the lower shoreface. Sand resources beyond the state/federal boundary offshore of northern Dare County were preliminarily assessed by Hoffman (1998). Four primary areas with potential for sand resources were identified and very roughly and conservatively estimated as containing at least 77 million cubic yards (Fig. 22). Three additional areas, considered of secondary interest due to their distance and water depth, were also delineated. This assessment pre-dated the analysis and development of the stratigraphic framework presented above. It did, however, rely on interpreted seismic profiles of the same lines presented here (S.W. Snyder, unpublished partial deliverable under contract to the NCGS) and the vibracore textural data analyses.

The earlier report (Hoffman, 1998) targeted the N-S oriented linear topographic highs (shoals) as the areas having the greatest potential for sand resources and steered away from the paleofluvial channels. One of the target areas is the seaward extension of the COE $S_1$ proposed borrow site; the others are detached (from the shoreface) shoal features, some of which overlie and thus postdate the paleofluvial system. The present analysis does not change this basic model.

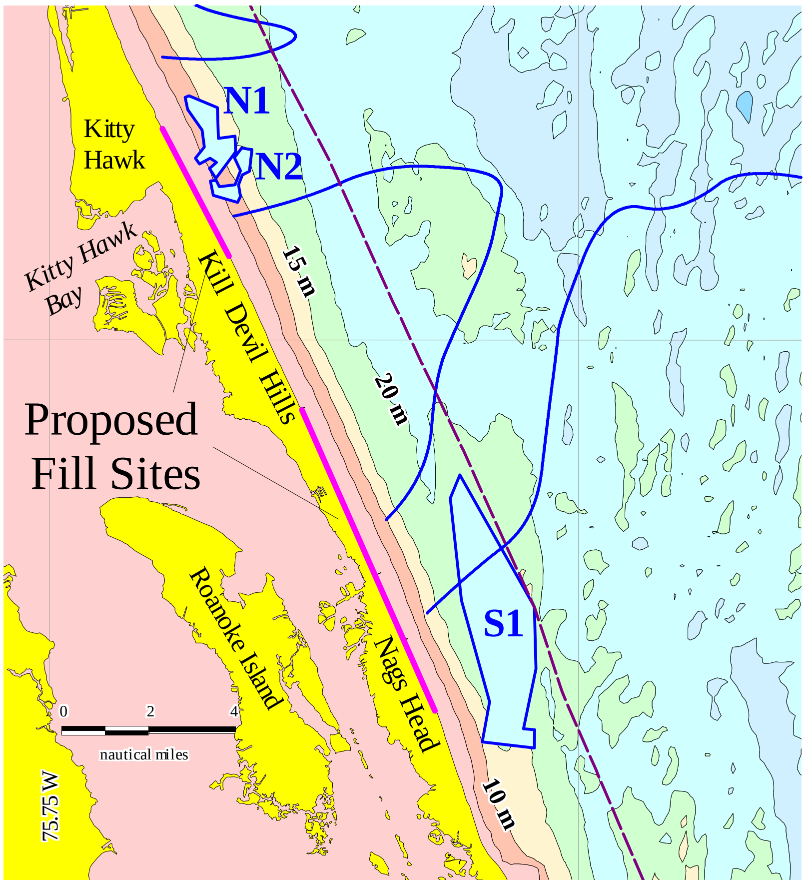


Figure 22. Northern dare project fill and proposed offshore borrow areas $S_1$, $N_1$, and $N_2$ which are reported to contain 104.5, 5.2, and 2.4 million cubic yards of sand, respectively (USACOE, personnal communication). The paleofluvial system outline is shown as well. Bathymetric contour interval is 5 m.

The four targets identified earlier remain; however, they are redrawn here to reflect the analysis and interpretation made in this study. Current GIS tools and bathymetric data also provide for refinement of the areas and the volumetric calculations.

Volume estimates can be made following the method described in Boss and Hoffman (1999 a-d; 2000) of using GIS software to measure the area bounded by a given unit thickness (isopach line) and multiply that area by the contour interval. Volumetric estimates of each contour interval can then be summed to give the total sediment amount. Table 3 below shows the sediment volumes estimated for each of the four primary potential resource areas.

Table 3..Size and potential sand resource volumetric estimates (in million cubic yards) for the four primary potential sand resource areas.

| Potential Resource Area | Size (Myds$^2$) | Volume (Myds$^2$) |
|---|---|---|
| Area 1 | 46.12 | 173.5 |
| Area 2 | 9.47 | 44.9 |
| Area 3 | 19.91 | 64.7 |
| Area 4 | 12.52 | 23.2 |
| | **88.02** | |
| **Totals** | | **306.3** |

Figure 23 shows the revised areas in a 3-D view along with the sand resource areas identified by the USACOE for the Dare County project. Note how the northern two COE areas lie on the lower shoreface. There is also a limited quantity of sand resource in these proposed sites. These borrow sites are expected to be exhausted after the initial construction phase, and the COE plans to use the $S_1$ site to maintain the northern project (COE, personal communication).

The minimum distance from the $S_1$ area to the northern project is 8.2 miles. By comparison, area 1 identified in the OCS by this report is a minimum of 4 miles to the northern project. Everything else being equal, the closer proximity of the OCS site would make it economically favorable to use for the northern project. Factors that would likely work against the OCS site being economically favorable versus the $S_1$ site would be the water depth of the OCS deposit and the fact that a single dredge could more or less remain on station in the $S_1$ site and supply fill material to both project areas.

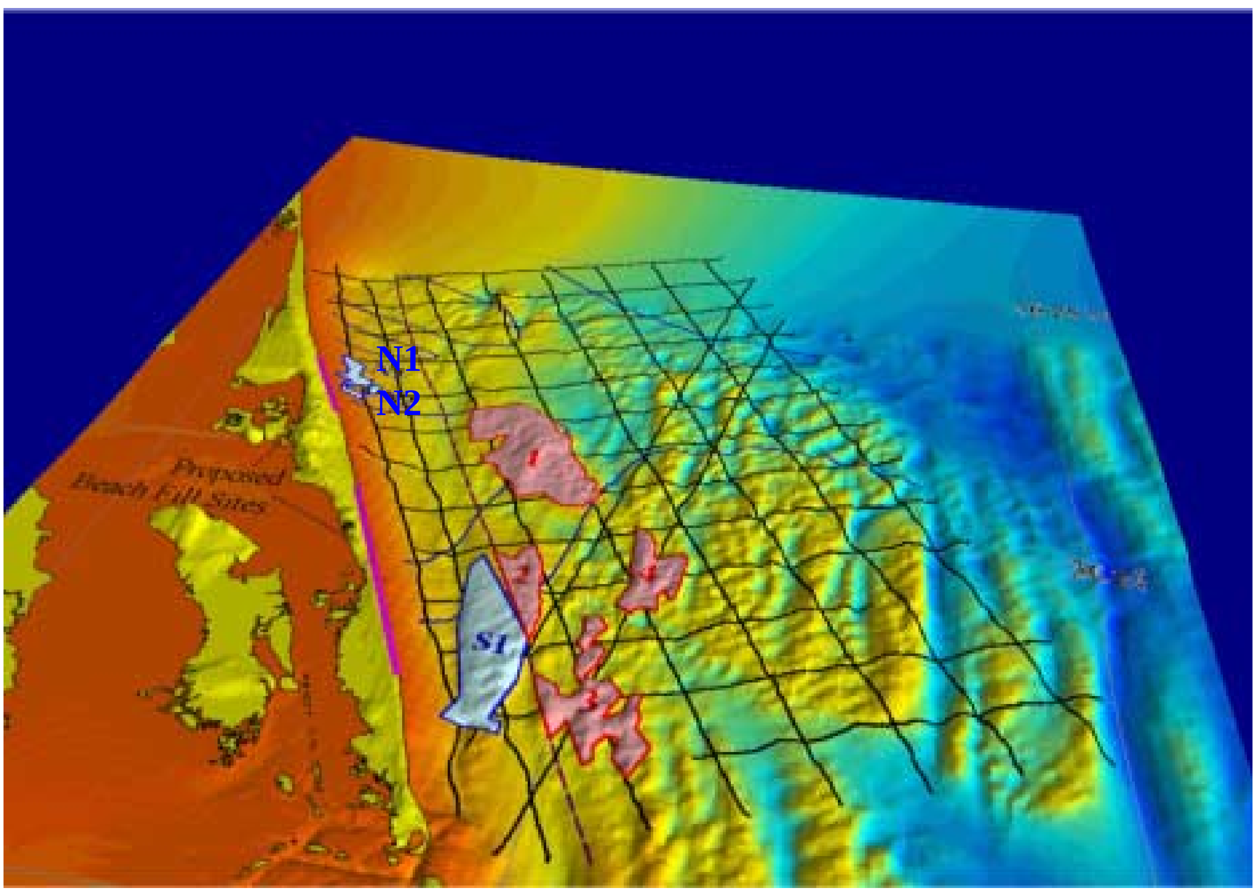


Figure 23. Perspective view (azimuth = 170°; viewing angle= 40°) showing position on inner shelf of proposed borrow sites for the northern Dare project and the four potential resource areas identified initially in Hoffman (1998) and refined here.

## Acknowledgements

This project spanned over 6 years until completion of this report. So numerous staff of the NCGS played roles at one time or another in the work. Bob Brooks, NCGS Geologist, and Amy Keyworth, NCGS Geologic Technician, each made significant contributions in organizing the data for this report. Mr. Brooks will be a producing a companion CD-ROM product for release as an NCGS Open-File Report. Bronwyn Kelly, NCGS Geologist in 1997-98 was responsible for core handling, descriptions, and textural data analyses. Tony Giordano and Carol Hartgen of MMS INTERMAR are acknowledged for their patience with the NCGS as we have encountered setbacks through the years that prevented earlier delivery of this report.

## REFERENCES CITED

Bellis, V., O'Connor, M.P., and Riggs, S.R., 1975, Estuarine shoreline erosion in the Albemarle-Pamlico region of North Carolina: North Carolina Sea Grant Publication UNC-SG-75-29, 67p.

Bloom, A.L., Broecker, W.S., Chappell, J., Matthews, R.K., and Mesolella, K.J., 1974, Quaternary sea level fluctuations on a tectonic coast: new $^{230}Th/^{234}U$ dates from the Hon Peninsula, New Guinea: Quaternary Research, v.4, p.185-205.

Boss, S.K., and Hoffman, C.W., 2000, Sand resources of the North Carolina Outer Banks:Final report [unpublished]: Contract report prepared for the Outer Banks Transportation Task Force and the North Carolina Department of Transportation, 87p.

Boss, S.K., and Hoffman, C.W., 1999a, Sand resources of the North Carolina Outer Banks 1st interim report: assessment of the Diamond Shoals study area[unpublished]: Contract report prepared for the Outer Banks Transportation Task Force and the North Carolina Department of Transportation, 26p.

Boss, S.K., and Hoffman, C.W., 1999b, Sand resources of the North Carolina Outer Banks 2nd interim report[unpublished]: assessment of the Buxton study area, Contract report prepared for the Outer Banks Transportation Task Force and the North Carolina Department of Transportation, 27p.

Boss, S.K., and Hoffman, C.W., 1999c, Sand resources of the North Carolina Outer Banks 3rd interim report[unpublished]: assessment of the Frisco-Ocracoke study area, Contract report prepared for the Outer Banks Transportation Task Force and the North Carolina Department of Transportation, 32p.

Boss, S.K., and Hoffman, C.W., 1999d, Sand resources of the North Carolina Outer Banks 4th interim report: assessment of the Pea Island study area[unpublished], Contract report prepared for the Outer Banks Transportation Task Force and the North Carolina Department of Transportation, 38p.

Boss, S.K. and Hoffman, C.W., 1997, Areas of potential sand resources in federal waters off the Outer Banks of North Carolina: Preliminary findings[unpublished]: report to United States Minerals Management Service/State of North Carolina Sand Resources Task Force, March 1997, 10p.

Boss, S.K. and Hoffman, C.W., and Riggs, S.R., 1999, Interpretation of side-scan sonar records of a portion of the inner North Carolina Continental Shelf between Oregon Inlet and Kitty Hawk[unpublished]: contract report to United States Minerals Management Service/State of North Carolina Sand Resources Task Force, January, 1999, 18p.

Chappell, K.J., 1983, A revised sea-level record for the last 300,000 years from Papua New Guinea: Search, v.14, p.99-101.

Chappell, K.J., 1974, Geology of coral terraces, Huon Peninsula, New Guinea: Geological Society of America Bulletin, v.85, p.553-570.

Dawson, A.G., 1992, Ice age Earth: Late Quaternary geology and climate: New York, Routledge, 293p.

Dresser Atlas Industries, Inc, 1982, Well logging and interpretation techniques: The course for home study: Dresser Atlas Industries, Inc., 228 p.

Eames, G.B., 1983, The late Quaternary seismic stratigraphy, lithostratigraphy, and geologic history of a shelf-barrier-estuarine system, Dare County, North Carolina: M.S. Thesis, Department of Geology, East Carolina University, Greenville, NC, 196p.

Fairbanks, R.G., 1989; A 17,000-year glacio-eustatic sea-level record: Influence of glacial melting rates on the Younger Dryas event and deep-ocean circulation: Nature, v.342, p.637-642.

Folk, R.L., 1964, Petrology of Sedimentary Rocks, Hemphill Publishing Company, Austin, TX, 182 p.

Hoffman, C.W., 1998, Preliminary assessment of potential sand resource areas offshore Nags Head, Kitty Hawk, and Kill Devil Hills, North Carolina [unpublished]: report to United States Minerals Management Service/State of North Carolina Sand Resources Task Force, April 1998, 12p.

Krumbein, W.C., 1934, Size frequency distribution of sediments: Journal of Sedimentary Petrology, v 4, p 65-77.

O'Connor, M.P., Riggs, S.R., and Winston, D., 1973, Recent estuarine sediment history of the Roanoke Island area, North Carolina: In B.W. Nelson (ed.), Environmental framework of coastal plain estuaries: Geological Society of America Memoir 133, p.453-464.

Pettijohn, F.J., 1975, Sedimentary Rocks, 3rd Edition: New York, Harper-Row Publishers, 627 p.

Riggs, S.R., 1996, Sediment evolution and habitat function of organic-rich muds within the Albemarle estuarine system, North Carolina: Esutaries, v.19, p.169-185.

Riggs, S.R., Snyder, S.W., Hine, A.C., and Mearns, D.L., 1996, Hardbottom morphology and relationship to the geologic framework: Mid-Atlantic continental shelf: Journal of Sedimentary Research, v.66, p.830-846.

Riggs, S.R., Ambrose, W.G., Jr., Cook, J.W., Snyder, Scott W., and Snyder, Stephen W., 1998, Sediment production on sediment-starved continental margins: The interrelationship between hardbottoms, sedimentological and benthic community processes, and storm dynamics: Journal of Sedimentary Research, v.68, p. 155-168.

Riggs, S.R., Cleary, W.J., and Snyder, S.W., 1995, Influence of inherited geologic framework on barrier shoreface morphology and dynamics: Marine Geology, v. 126, p.213-234.

Riggs, S.R., York, L.L., Wehmiller, J.F., and Snyder, S.W., 1992, Depositional patterns resulting from high-frequency Quaternary sea-level fluctuations in northeastern North Carolina: In Fletcher, C.H. and Wehmiller, J.F. (eds.), Quaternary coasts of the United States: Marine and lacustrine systems: Society of Economic Paleontologists and Mineralogists Special Publication 48, p.141-153.

Riggs, S.R. and Belknap, D.K., 1988, Upper Cenozoic processes and environments of the continental margin sedimentation: Eastern United States: In Sheridan, R.E. and Grow, J.A. (eds.), The Atlantic continental margin of the United States: Geology of North America, Geological Survey of America Decade of North American Geology v.I-2, p.131-176.

Riggs, S.R. and O'Connor, M.P., 1974, Relict sediment deposits in a major transgressive coastal system: North Carolina Sea Grant Publication UNC-SG-74-04, 37p.

Schlee, J.S., Manspeiser, W., and Riggs, S.R., 1988, Paleoenvironments offshore Atlantic U.S.margin: In Sheridan, R.E. and Grow, J.A. (eds.), The Atlantic continental margin of the United States: Geology of North America, Geological Survey of America Decade of North American Geology v.I-2, p.365-385

Shackleton, N.J., 1987, Oxygen isotopes, ice volume and sea level: Quaternary Science Reviews, v.6, p.15-17.

Snyder, S.W., 1993, North Carolina Outer Banks beach nourishment sand resource study, first interim report: Shallow, high-resolution seismic survey, offshore Nags Head area: North Carolina Geological Survey Open-File Report 93-38, 47p.

Wehmiller, J.F., York, L.L., Bart, M.L., 1995, Amino acid racemization geochronology of reworked Quaternary mollusks on U.S. Atlantic coast beaches: implications for chronostraigraphy, taphonomy, and coastal sediment transport: Marine Geology, v.124, p.303-337.

York, L.L., Wehmiller,J.F., Cronin, T.M., and Ager, T.A., 1989, Stetson Pit, Dare County, North Carolina: An integrated chronologic, faunal, and floral record of subsurface coastal sediments: Palaeogeography, Palaeoclimatelogy, and Palaeoecology, v.72, p.115-132.

# APPENDIX 1. Basic Information for Each Vibracore.

| Core | Length (m) | $H_2O$ (m) | $H_2O$ (ft) | Lat | Long | Mean GS (Φ) | Std. Dev. (Φ) | Mean GS (mm) | % Sand | % Mud | % Grv |
|---|---|---|---|---|---|---|---|---|---|---|---|
| MMS-001 | 4.75 | 22.5 | 68 | 35.872967 | -75.479467 | 1.66 | 1.31 | 0.32 | 85.6 | 4.0 | 10.1 |
| MMS-002A | 5.69 | 20.8 | 63 | 35.903633 | -75.495083 | 1.78 | 1.11 | 0.29 | 81.0 | 10.7 | 7.9 |
| MMS-003 | 4.99 | 22.8 | 69 | 35.889667 | -75.517967 | 2.72 | 1.38 | 0.15 | 64.7 | 30.5 | 4.3 |
| MMS-004 | 6.02 | 20.1 | 61 | 35.945667 | -75.576517 | 2.91 | 1.35 | 0.13 | 67.1 | 29.3 | 3.0 |
| MMS-005 | 4.77 | 23.1 | 70 | 35.930967 | -75.520050 | 1.26 | 1.20 | 0.42 | 80.1 | 4.0 | 15.6 |
| MMS-007 | 5.85 | 23.1 | 70 | 35.985267 | -75.570250 | 2.55 | 0.99 | 0.17 | 63.8 | 29.9 | 5.9 |
| MMS-008 | 3.83 | 24.8 | 75 | 36.011417 | -75.597617 | 2.33 | 1.22 | 0.20 | 58.2 | 38.4 | 3.2 |
| MMS-009 | 5.64 | 20.1 | 61 | 36.005267 | -75.515450 | 2.48 | 0.76 | 0.18 | 93.4 | 5.7 | 0.4 |
| MMS-010 | 5.79 | 24.8 | 75 | 36.037750 | -75.527133 | 2.81 | 0.91 | 0.14 | 77.1 | 22.0 | 0.5 |
| MMS-011 | 5.95 | 29.1 | 88 | 36.045433 | -75.505617 | 2.11 | 1.37 | 0.23 | 69.8 | 17.3 | 12.4 |
| MMS-012 | 5.36 | 22.5 | 68 | 36.053683 | -75.583850 | 2.27 | 1.12 | 0.21 | 66.2 | 22.6 | 11.0 |
| MMS-013 | 2.32 | 28.4 | 86 | 36.087467 | -75.515067 | 2.40 | 0.89 | 0.19 | 91.7 | 7.0 | 0.6 |
| MMS-014A | 5.94 | 25.4 | 77 | 36.096583 | -75.570300 | 3.70 | 0.73 | 0.08 | 53.0 | 46.6 | 0.0 |
| MMS-015 | 4.06 | 24.4 | 74 | 36.092133 | -75.580433 | 4.05 | 0.55 | 0.06 | 31.3 | 68.4 | 0.0 |
| MMS-016 | 6.02 | 24.4 | 74 | 36.087883 | -75.590417 | 3.52 | 0.82 | 0.09 | 56.8 | 42.8 | 0.0 |
| MMS-017 | 5.97 | 22.5 | 68 | 36.084767 | -75.601750 | 3.33 | 0.81 | 0.10 | 52.9 | 45.8 | 1.0 |
| MMS-018 | 4.17 | 25.1 | 76 | 36.078267 | -75.617300 | 4.00 | 0.72 | 0.06 | 33.7 | 65.3 | 0.7 |
| MMS-019 | 5.95 | 21.5 | 65 | 36.105733 | -75.645733 | 3.79 | 0.59 | 0.07 | 45.2 | 53.6 | 0.0 |
| MMS-020 | 5.99 | 22.8 | 69 | 36.117300 | -75.611717 | 2.94 | 1.14 | 0.13 | 65.7 | 32.7 | 1.3 |
| MMS-021 | 5.75 | 26.4 | 80 | 36.147383 | -75.530250 | 3.03 | 0.84 | 0.12 | 77.2 | 22.0 | 0.6 |
| MMS-022 | 3.21 | 22.5 | 68 | 36.138450 | -75.655350 | 2.51 | 1.34 | 0.18 | 66.3 | 23.2 | 10.2 |
| MMS-023 | 3.75 | 22.5 | 68 | 36.163517 | -75.587633 | 2.40 | 0.75 | 0.19 | 96.0 | 3.7 | 0.1 |
| MMS-024 | 5.61 | 22.5 | 68 | 36.167017 | -75.576750 | 2.70 | 0.77 | 0.15 | 86.4 | 11.8 | 1.5 |
| MMS-025 | 4.59 | 24.1 | 73 | 36.177833 | -75.650317 | 2.94 | 1.72 | 0.13 | 38.0 | 48.0 | 13.8 |
| MMS-026 | 5.85 | 16.8 | 51 | 36.188667 | -75.721300 | 2.45 | 1.17 | 0.18 | 57.9 | 29.5 | 12.5 |
| MMS-027 | 3.59 | 23.1 | 70 | 36.202067 | -75.681400 | 2.65 | 1.03 | 0.16 | 73.2 | 26.4 | 0.1 |
| MMS-028 | 4.17 | 23.1 | 70 | 36.213833 | -75.652500 | 3.98 | 0.58 | 0.06 | 28.8 | 70.7 | 0.3 |
| MMS-029 | 1.71 | 25.8 | 78 | 36.217317 | -75.641933 | 3.57 | 0.65 | 0.08 | 65.6 | 34.0 | 0.1 |
| MMS-030 | 4.55 | 27.4 | 83 | 36.186417 | -75.623983 | 2.85 | 1.22 | 0.14 | 53.6 | 34.1 | 12.0 |
| MMS-031 | 3.27 | 21.8 | 66 | 36.188950 | -75.617717 | 2.83 | 0.78 | 0.14 | 83.4 | 15.8 | 0.7 |
| MMS-032 | 4.51 | 18.8 | 57 | 36.191517 | -75.611417 | 2.23 | 0.89 | 0.21 | 95.7 | 2.8 | 1.7 |
| MMS-033B | 2.17 | 29.7 | 90 | 36.232483 | -75.598750 | 3.59 | 0.79 | 0.08 | 63.6 | 36.1 | 0.2 |
| MMS-034 | 5.18 | 29.7 | 90 | 36.240183 | -75.577267 | 3.19 | 1.29 | 0.11 | 44.9 | 48.0 | 6.7 |
| MMS-035 | 6.00 | 28.4 | 86 | 36.204633 | -75.576133 | 2.98 | 1.44 | 0.13 | 52.8 | 40.3 | 6.5 |
| MMS-036 | 5.93 | 27.7 | 84 | 36.203167 | -75.578383 | 2.84 | 1.12 | 0.14 | 70.2 | 25.3 | 4.3 |
| MMS-037 | 3.37 | 29.7 | 90 | 36.197050 | -75.529350 | 2.55 | 1.18 | 0.17 | 79.7 | 13.4 | 6.8 |

Appendix 1. (continued)

| Core | Length (m) | $H_2O$ (m) | $H_2O$ (ft) | Lat | Long | Mean GS (Φ) | Std. Dev. (Φ) | Mean GS (mm) | % Sand | % Mud | % Grv |
|---|---|---|---|---|---|---|---|---|---|---|---|
| MMS-038 | 5.91 | 29.7 | 90 | 36.214233 | -75.494833 | 3.31 | 0.97 | 0.10 | 54.6 | 44.7 | 0.7 |
| MMS-039 | 6.04 | 32.7 | 99 | 36.257667 | -75.474283 | 3.19 | 1.47 | 0.11 | 43.8 | 52.4 | 4.0 |
| MMS-040 | 5.04 | 29.7 | 90 | 36.210450 | -75.461367 | 2.34 | 0.68 | 0.20 | 96.3 | 3.6 | 0.3 |
| MMS-041 | 5.68 | 30.1 | 91 | 36.170700 | -75.467517 | 3.12 | 1.09 | 0.12 | 63.8 | 31.8 | 4.1 |
| MMS-042 | 2.71 | 26.1 | 79 | 36.127750 | -75.480717 | 2.58 | 0.71 | 0.17 | 95.7 | 4.1 | 0.1 |
| MMS-043 | 5.73 | 29.7 | 90 | 36.124017 | -75.497367 | 3.49 | 0.77 | 0.09 | 66.5 | 33.4 | 0.1 |
| MMS-044 | 4.65 | 24.4 | 74 | 36.105817 | -75.523217 | 2.58 | 0.62 | 0.17 | 96.3 | 3.2 | 0.0 |
| MMS-045 | 6.06 | 26.8 | 81 | 36.087817 | -75.489750 | 3.35 | 0.89 | 0.10 | 63.8 | 35.9 | 0.1 |
| MMS-046 | 5.99 | 30.7 | 93 | 36.070550 | -75.457800 | 2.07 | 1.00 | 0.24 | 82.7 | 9.7 | 7.4 |
| MMS-047 | 5.69 | 25.1 | 76 | 36.008817 | -75.469583 | 2.11 | 0.79 | 0.23 | 94.5 | 3.6 | 1.4 |
| MMS-048 | 6.04 | 30.1 | 91 | 36.031433 | -75.444017 | 2.08 | 0.85 | 0.24 | 88.8 | 9.8 | 0.7 |
| MMS-049 | 5.92 | 25.8 | 78 | 36.033350 | -75.438520 | 2.33 | 0.98 | 0.20 | 83.2 | 14.7 | 1.7 |
| MMS-050 | 4.42 | 26.1 | 79 | 36.060350 | -75.362750 | 2.33 | 0.60 | 0.20 | 98.1 | 1.7 | 0.1 |
| MMS-051 | 5.91 | 26.8 | 81 | 36.011850 | -75.380683 | 2.45 | 0.82 | 0.18 | 90.7 | 7.6 | 1.4 |
| MMS-052 | 5.97 | 29.7 | 90 | 35.970950 | -75.402117 | 3.24 | 0.78 | 0.11 | 61.4 | 38.9 | 0.0 |
| MMS-053 | 6.07 | 21.5 | 65 | 35.937583 | -75.429200 | 2.35 | 0.72 | 0.20 | 97.4 | 4.2 | 0.4 |
| MMS-054 | 5.25 | 23.1 | 70 | 35.905450 | -75.412317 | 2.37 | 0.62 | 0.19 | 97.3 | 2.4 | 0.2 |
| MMS-055 | 5.09 | 20.8 | 63 | 35.895983 | -75.360600 | 1.84 | 0.69 | 0.28 | 97.7 | 1.2 | 0.5 |
| MMS-056 | 5.71 | 25.4 | 77 | 35.889350 | -75.344817 | 2.53 | 0.60 | 0.17 | 96.2 | 2.3 | 1.2 |
| MMS-057 | 4.56 | 23.4 | 71 | 35.898317 | -75.269850 | 2.26 | 0.62 | 0.21 | 97.6 | 1.5 | 0.4 |
| **minimum** | 1.71 | 16.84 | 51.00 | | | 1.26 | 0.55 | 0.06 | 28.84 | 1.20 | 0.01 |
| **maximum** | 6.07 | 32.69 | 99.00 | | | 4.05 | 1.72 | 0.42 | 98.12 | 70.74 | 15.56 |
| **average** | 5.01 | 25.10 | 76.02 | | | 2.75 | 0.94 | 0.16 | 72.09 | 24.44 | 3.23 |

Note: Mean Grain Size (GS) was determined statistically after (Folk, 1964). The mean GS (mm) is a conversion of the phi (Ø) value.

**APPENDIX 2 Histograms showing grain size distribution for whole vibracores.**

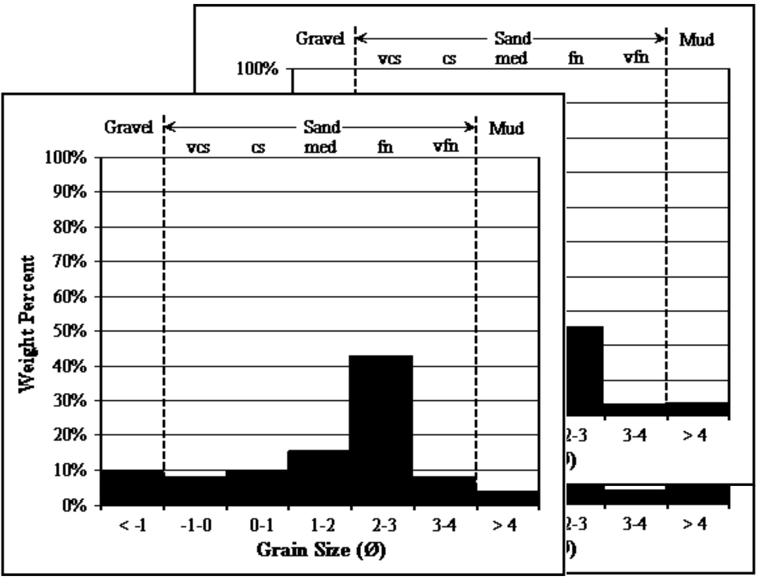


**MMS-002**

**MMS-002A**

**MMS-003**

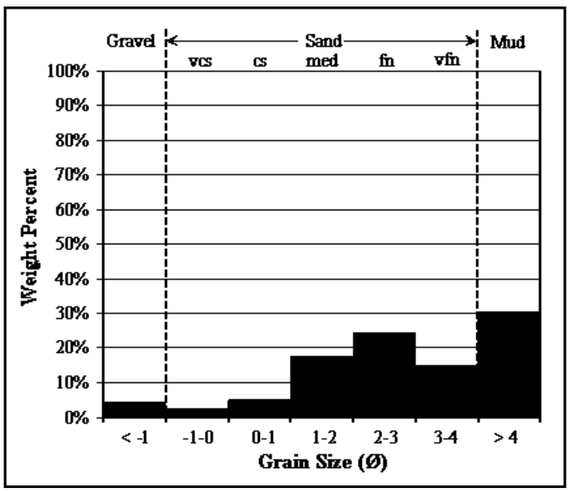


**MMS-004**

**MMS-005**

Appendix 2 Histograms showing grain size distribution for whole vibracores (continued).

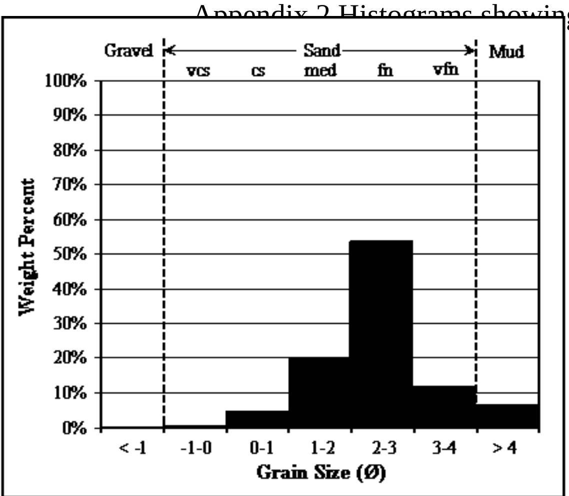


**MMS-009**

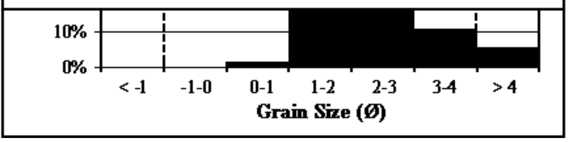


**MMS-0010**

**MMS-011**

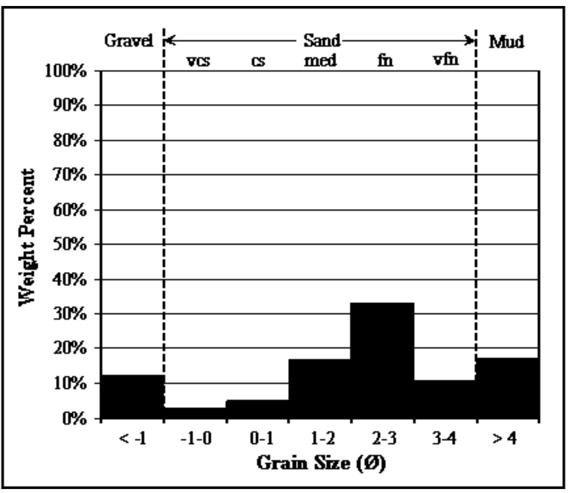


**MMS-012**

**MMS-013**

Appendix 2 Histograms showing grain size distribution for whole vibracores (continued).

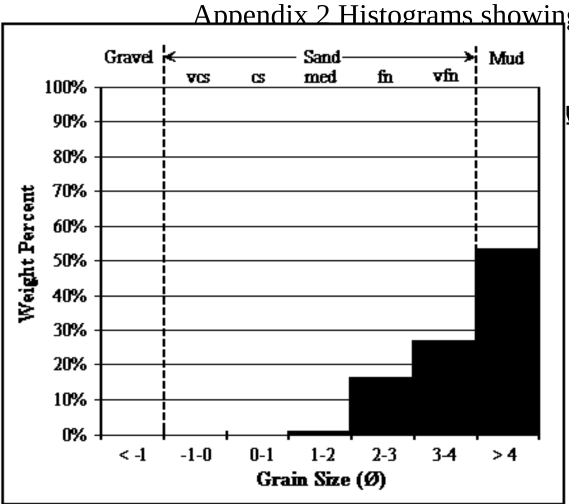


A

**MMS-015**

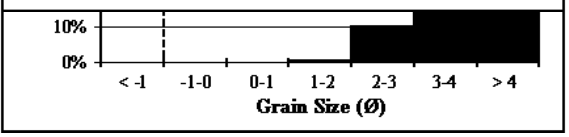


**MMS-016**

**MMS-017**

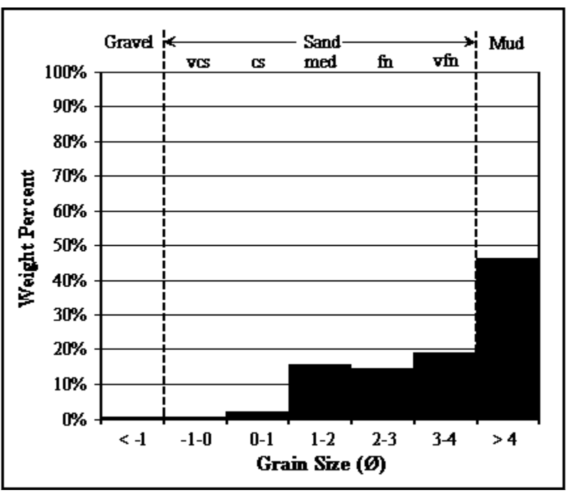


**MMS-018**

**MMS-019**

Appendix 2 Histograms showing grain size distribution for whole vibracores (continued).

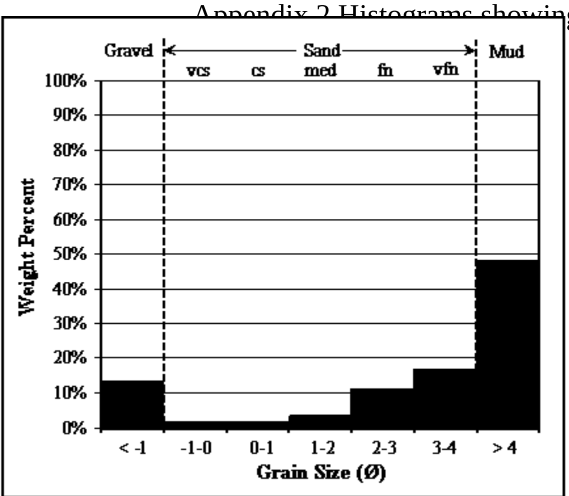


**MMS-021**

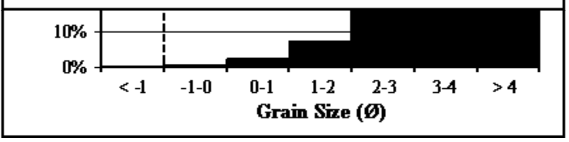


**MMS-022**

**MMS-023**

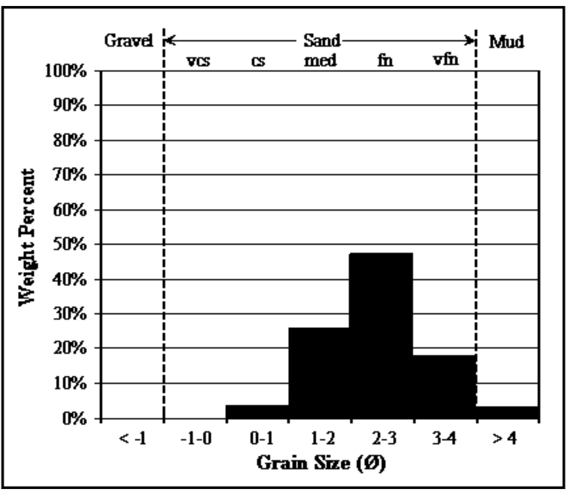


**MMS-024**

**MMS-025**

Appendix 2 Histograms showing grain size distribution for whole vibracores (continued).

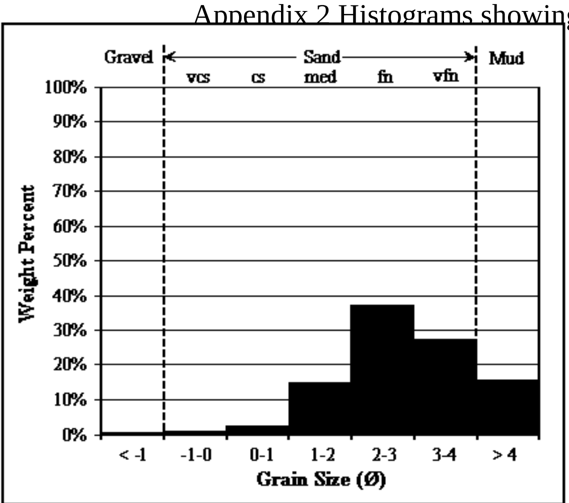


**MMS-027**

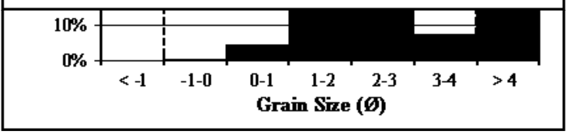


**MMS-028**

**MMS-029**

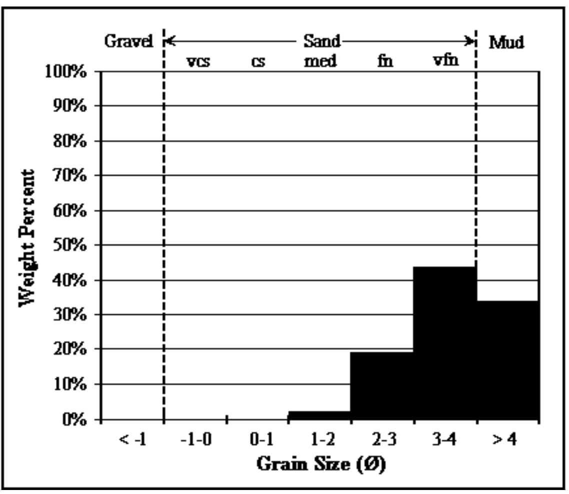


**MMS-030**

**MMS-031**

Appendix 2 Histograms showing grain size distribution for whole vibracores (continued).

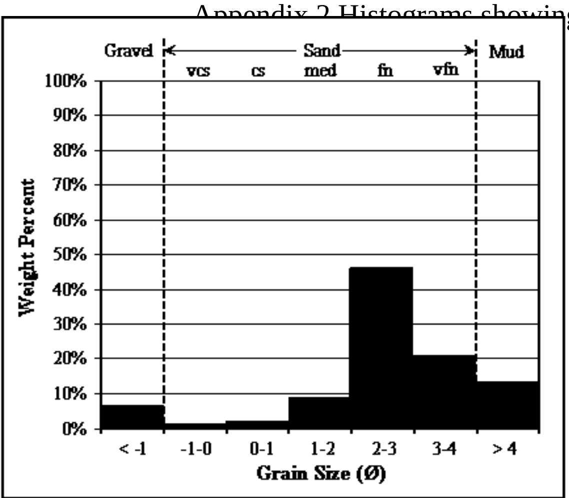


**MMS-033B**

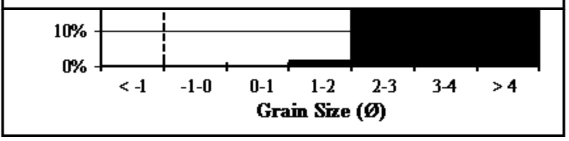


**MMS-034**

**MMS-035**

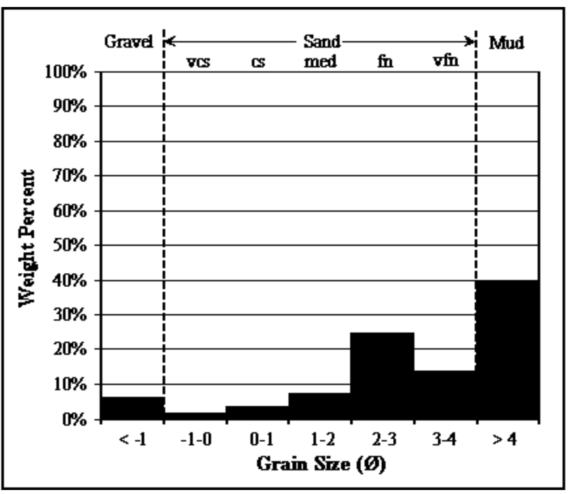


**MMS-036**

**MMS-037**

Appendix 2 Histograms showing grain size distribution for whole vibracores (continued).

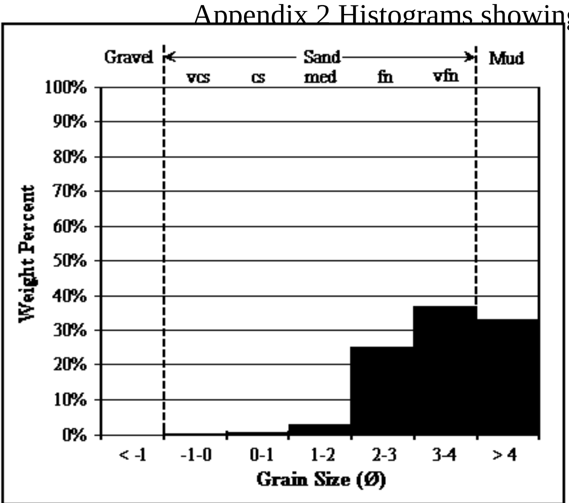


**MMS-039**

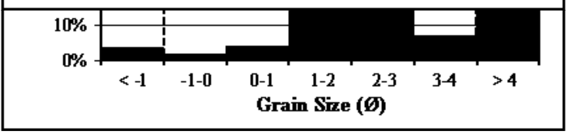


**MMS-040**

**MMS-041**

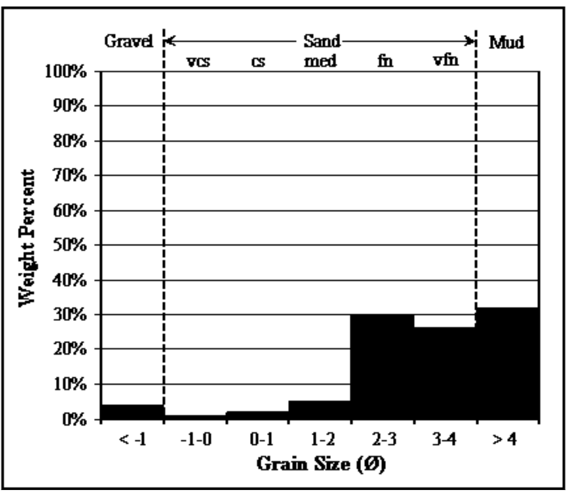


**MMS-042**

**MMS-043**

Appendix 2 Histograms showing grain size distribution for whole vibracores (continued).

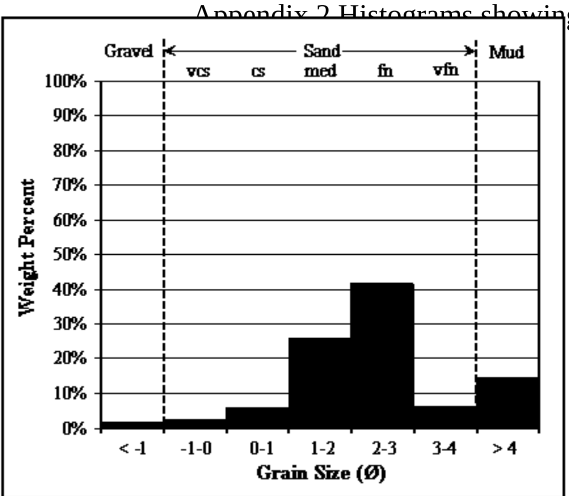


**MMS-045**

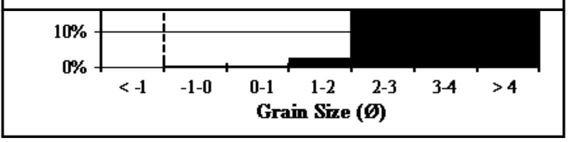


**MMS-046**

**MMS-047**

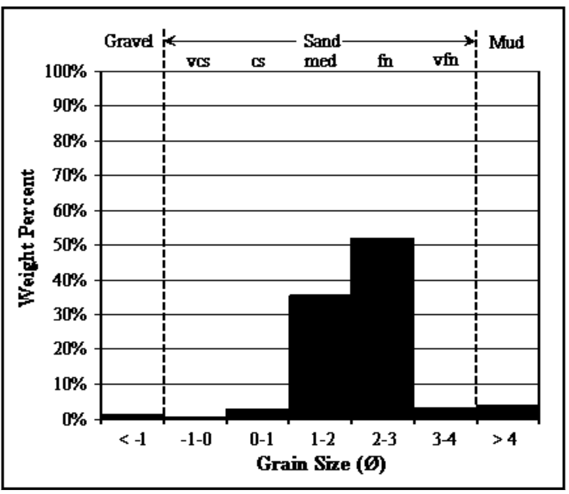


**MMS-048**

**MMS-049**

Appendix 2 Histograms showing grain size distribution for whole vibracores (continued).

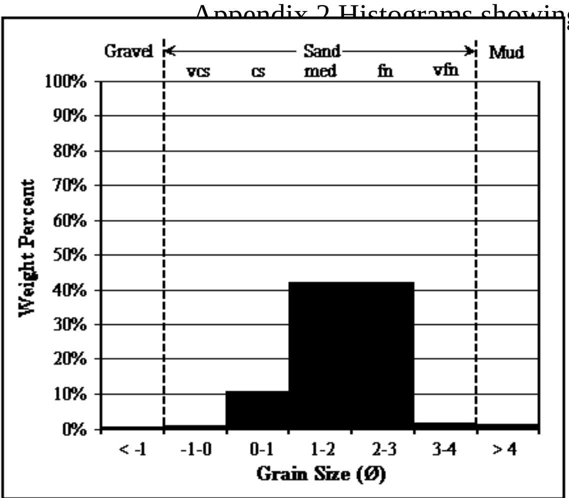


MMS-051

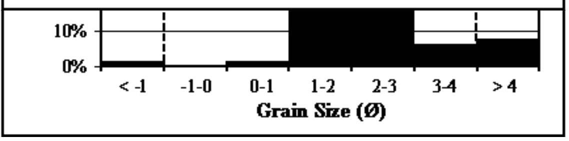


MMS-052

MMS-053

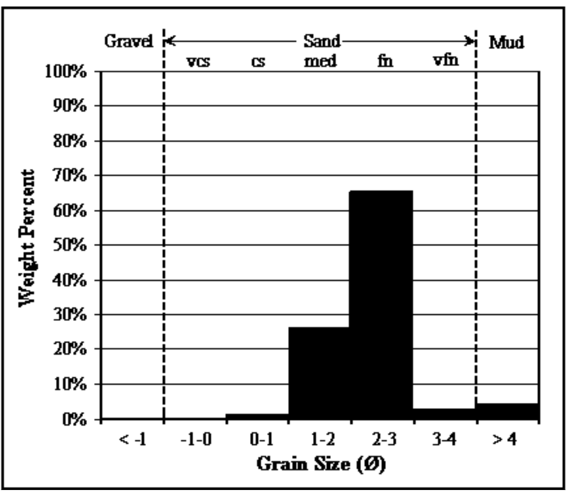


MMS-054

MMS-055

Appendix 2 Histograms showing grain size distribution for whole vibracores (continued).

## MMS-056

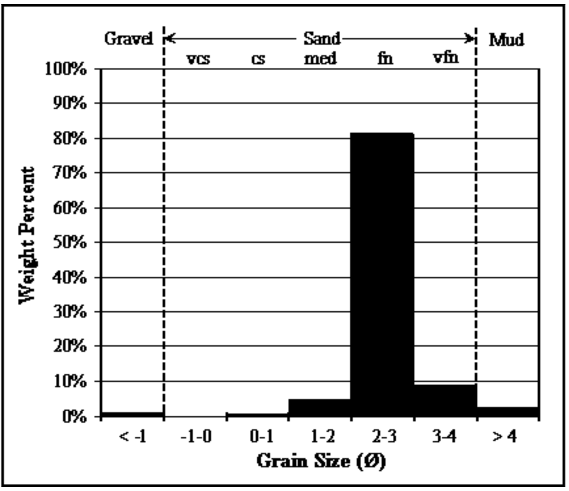


## MMS-057